Hypertemporal Vegetation Classification for Flood Hazard Assessment.

Othusitse Lekoko

February, 2010

Hypertemporal Vegetation Classification for Flood Hazard Assessment

by

Othusitse Lekoko

Thesis submitted to the International Institute for Geo-information Science and Earth Observation in partial fulfilment of the requirements for the degree of Master of Science in Geo-information Science and Earth Observation, Specialisation: Applied Earth Sciences (Geo-Hazards)

Thesis Assessment Board

Prof. Dr. Victor Jetten
Board Chairman – Applied Earth Sciences (ITC, Netherlands)
Dr. E. A. Addink
External Examiner – Faculty of Earth Sciences (Utrecht University, Netherlands)
Dr. Menno Straatsma
1st Supervisor – Applied Earth Sciences (ITC, Netherlands)
Dr. Ir. Anton Vrieling
2nd Supervisor – Natural Resources Management (ITC, Netherlands)
Drs. Tom Loran
Observer - Applied Earth Sciences (ITC, Netherlands)

**INTERNATIONAL INSTITUTE FOR GEO-INFORMATION SCIENCE AND EARTH OBSERVATION
ENSCHEDE, THE NETHERLANDS**

Disclaimer

This document describes work undertaken as part of a programme of study at the International Institute for Geo-information Science and Earth Observation. All views and opinions expressed therein remain the sole responsibility of the author, and do not necessarily represent those of the institute.

Abstract

Floodplain vegetation, its structure and growth properties, affect flow and flood wave propagation during flood events. To estimate the impact of vegetation on the flow resistance, flow conditions are determined for different conditions and properties of vegetation. Traditional methods to determine vegetation properties have mainly been ground based. These methods are proving to be insufficient because of the large spatial heterogeneity of floodplain vegetation. This study looks at remote sensing, specifically at hypertemporal satellite technology, as a promising resource for fast, efficient and more effective method of vegetation characterisation for flood hazard assessment. As a new and emerging field, it is still necessary to collect field data to validate the accuracy of the method, therefore Leaf Area Index (LAI) and landcover characterization were included as part of the study. Nineteen images were used over the Netherlands growing season of seven months. The two week time step between images was very critical not only because of possibility to miss important vegetation growth stages, but also because the floodplain under study has agricultural activities including cattle rearing, haymaking and maize farming which may have noticeable influence on landcover over a short period of time. A questionnaire was distributed amongst the farmers to capture these activities and it was found that most farmers plant their maize in May and harvest in September or October. Grass cutting for haymaking varied on a 4-8 week cycle between farmers, depending on the intensity of the farming activities in a particular farm. In all the cases the grass was left for meadow during the winter period.

The floodplain vegetation was classified using three different methods on a 19 layer hypertemporal NDVI stack; Maximum Likelihood Classification (MLC), Spectral Angle Mapper (SAM) and NDVI Based Profile matching. All the classifications performed below expectation with SAM lowest at 50.54% followed by MLC at 54.84%. The classification was benchmarked against the ecotope map which is has the accuracy of 69%. NDVI Profile matching was only assessed visually and no statistical evaluation was performed. The ISODATA output from the NDVI Profile classification showed the subtle differences within landcover that was classified as a unit in MLC and SAM showing potential to take advantage of the temporal dimension within the image stack. Landcover specific NDVI Profiles were produced with the use fieldwork data. The profiles displayed characteristic shape unique to each landcover type and even showed deflection points associated with cropping activities of particular landcover types. The study confirmed that the DMC images can produce landcover specific temporal profiles in the IJssel floodplain but landcover classification using these profiles is not practical.

Field measured LAI was related to NDVI without the use transformation coefficients and performed poorly with a low correlation coefficient, R^2 of 0.43 for maize, and almost no correlation for herbaceous vegetation for forest.

Keywords: *Flood Hazard, Hypertemporal, NDVI, DMC, vegetation roughness*.

Acknowledgements

First and foremost I would like to thank the Erasmus Mundus Lot 10 program for affording me the opportunity to pursue this MSc study with ITC/University of Twente in the Netherlands.

My sincere gratitude to my supervisors, Dr. Menno Straatsma and Dr. Ir. Anton Vrieling for the support and guidance they provided me throughout my research. I would also like to thank Drs. Ir. Kees de Bie for being my resource specialist. Many thanks to the whole Applied Earth Sciences department under the directorship of Drs. Tom Loran with unending support of Anneke Nikijuluw.

I would like to thank DMCii International (Pty) Ltd, UK for supplying us with the images used in this research at no cost.

To my wife Lisele, your love and support has kept me going throughout the 18months that I had to be away from my family pursuing this study. You have worked hard to take care of the family. And to my daughters Bokang and Rorisang this is for you, thank you for all the baby love, it made the difference in my life and study.

My whole extended family, my mother Mmantlha Lekoko, my siblings, the matriarch of the family Mmaeto Lekoko, and everyone who supported me throughout this challenging time I am grateful to you and may God Bless and keep you healthy always.

To my friends and course mates at ITC, it was the strength that we displayed together that got us all going. The discussions we held were very helpful and very valuable. There was no time anyone was too busy to help another, that's the spirit. We were a community, and let that community live within your hearts forever. All the best in your future endeavours.

I will not forget Mr. Eddie Aabobe whose simple forwarding of scholarship information started the ball rolling and saw me pack my bags for this MSc study in the Netherlands, thank you The Eddie man, may your blessings grow many folds.

~ ~ ~ ~ ~ In memory of Makabe Lekoko, Monaso Lekoko Midgley, Ofentse Lekoko – RIP~ ~ ~ ~ ~

Table of contents

List of figures

Landcover Picture Plates

List of tables

Acronyms

ALS	-	Airborne Laser Scanner
AVHRR	-	Advanced Very High Resolution Radiometer
CBERS	-	China-Brazil Earth Resources Satellite program
DEM	-	Digital Elevation Model
DMC	-	Disaster Management Constellation (Pty) Ltd.
EVI	-	Enhanced Vegetation Index
GCP	-	Ground Control Point
ISODATA	-	Iterative Self-Organized Data Analysis Technique
LAI	-	Leaf Area Index
LiDAR	-	Light Detection And Ranging
LDM	-	Leaf Dry Matter
LUT	-	Look Up Table
MERIS	-	MEdium Resolution Imaging Spectrometer
MODIS	-	MODerate-resolution Imaging Spectro-radiometer
MLC	-	Maximum Likelihood Classification
NASA	-	National Aeronautics and Space Administration
NDVI	-	Normalised Differentiation Vegetation Index
NIR	-	Near InfraRed
NOAA	-	National Oceanic and Atmospheric Administration
PCA	-	Principal Components Analysis
PIF	-	Pseudo Invariant Feature
SAM	-	Spectral Angle Mapper
SAVI	-	Soils Adapted Vegetation Index
SPOT	-	Satellite Pour l'Observation de la Terre
SRTM	-	Shuttle Radar Topography Mission
TOA	-	Top Of the Atmosphere

1. Introduction

1.1. Background

1.1.1. Flood hazard model input

Flooding has become a large environmental hazard with significant economic damage and human suffering. The importance of accurate predictions of flood behaviour cannot be over emphasised, it is essential to understand the hydrodynamic characteristics of the floodplain and their effects on flood modelling. In addition to surface topography, floodplain characteristics include vegetation roughness as a key input parameter in flood modelling (Straatsma and Baptist, 2008). But compared with topography, the specification of flow resistance due to vegetation is a far more ambiguous process (Horritt, 2006). Modern river management tries explicitly to combine flood defence with ecological integrity but at the same time ecological integrity leads to succession of vegetation and higher friction values. This succession also leads to a more spatiotemporal variation of vegetation which in turn requires monitoring and accurate characterization (Straatsma, 2007).

In the Netherlands, roughness mapping is based on floodplain vegetation types that were delineated from manual interpretation of the aerial photographs into what is termed the ecotope maps (refer section 2.3). Each of the ecotopes is assigned a value for vegetation height and density using a look up table (LUT). Many flood models used in the Netherlands use the ecotope maps along with the LUTs for vegetation roughness parameterization. The IJssel river management authority bases its management strategy on the ecotope maps. The current accuracy of the ecotope maps is estimated at 69% (Knotters and Brus, In press), therefore insufficient accuracy in the vegetation classification will result in flood modelling with large amount of uncertainty.

The Dutch government maintains the highest safety levels against flooding world-wide, with flooding design discharge of 2015 set to risks smaller than one per 1250 years(Straatsma and Alkema, 2009). To guarantee safety levels, flood-risk models must be updated every five years. This requires spatially explicit data on vegetation to derive hydraulic roughness parameters (Straatsma and Baptist, 2008) and for hydrodynamic models the vegetation roughness is one of the determining factors for the computed water levels.

1.1.2. Roughness

Floodplain roughness parameterization is one of the key elements of hydrodynamic modelling of river flow, which is directly linked to water levels that exceed embankments of lowland fluvial areas (Straatsma and Baptist, 2008). The contribution to floodplain roughness is mainly by vegetation thereofore is critical to account for the actual properties and dynamic changes of vegetation. In the IJssel river floodplain, willows can shoot up more than one metre per year after taking root at a location where it was formerly bare ground (Silva et al., 2001). As trees grow higher the general density of the vegetation increases and more plant material is deposited on the ground, further increasing the roughness.

The amount of vegetation material is quantified through resistance coefficients like the Manning $\boldsymbol{n}$, Chézy $\boldsymbol{C}$ and the Weisbach $\boldsymbol{f}$. All the coefficients have vegetation at the centre of their operation and there is no clear theoretical advantage of one coefficient over the others, however Yen (2002) refers to study by Lopez and Garcia (1997) that Manning $\boldsymbol{n}$ increases with vegetation density. Järvelä (2004) showcased the impact of leaf density by comparing predicted and measured friction factors for leafless and leafy willows and found that the discrepancies of f were 18% and 61% for the leafless and leafy cases, respectively. These findings suggest that LAI is a key component of resistance coefficients.

A number of methods to account for vegetation properties have widely been noted in research, however Szoszkiewicz *et al.* (2003) suggest that ground measurements are limited in spatial range due to the large spatial heterogeneity of floodplain vegetation structure. The authors further note that remote sensing techniques with very fast tools for large scale data acquisition promise an opportunity to resolve problem of data inadequacy caused by the inefficient field based methods of measuring vegetation properties.

1.1.3. Classification of vegetation for roughness parameterization

Remote sensing, specifically in the satellite technology, is one of the areas of development that has enabled researchers to efficiently and effectively collect key information about hazards and their associated disasters. Researchers have been able to study, characterise and to some extend predicted some of the phenomena with improved accuracy. Remote sensing is very sensitive to the surface characteristics of the object or area under investigation, resulting from the different spectral characteristics of different materials, and different sensors have been built that are especially suitable for specific surface materials (Kerle, 2009). The Disaster Monitoring Constellation (DMC) satellites are some of the sensors that are designed for and dedicated to monitoring of hazards and disasters around the world. It provides imagery for rapid response to disasters providing both medium spatial (32m) and high temporal (up-to 1day for specific arrangements) resolution with a swath width of 324km. While the technological advances in remote sensing has enabled high resolution in satellite data trend analysis of satellite observations is subject to error, and even ecosystem change can be confused with inter-annual variability (Bradley and Mustard, 2008). Szoszkiewicz *et al.* (2003) claims that the increased availability of high resolution satellite data makes the analysis of large floodplains possible but makes no reference as to whether high resolution also means larger swath angle for many satellites.

1.1.4. Multitemporal RS and new application to floodplain vegetation

The periodic acquisition of remotely sensed data at short temporal intervals is an efficient way to monitor the seasonal and inter annual development of land surfaces (Geerken, 2009). The author further asserts that the use of NDVI time series data can identify biophysical characteristics, landuse practices, and even recognize particular landcover types. De Bie *et al.* (2008) used NDVI profiles to identify the extent and nature of land cover units in Portugal; to monitor flooded areas and to map gradients in Mozambique, the Limpopo valley; to detect spatial differences in water availability in Garmsar, Iran; to link NDVI profiles to land use classes in Nizamabad, India, and to disaggregate reported agricultural crop statistics to 1x1km pixel crop maps in Andalucía, Spain. However throughout this work the authors depended on visual profile matching . The advantage was that the variation in behaviour between profiles was considerably large (de Bie *et al.*, 2008). Geerken (2009) used an algorithm to recognize NDVI time series cycle and curve shape to classify the vegetation types. However the method required a reference profile on which the new classification would be based on.

1.2. Research Problem

Many researchers have used satellite data with high temporal properties like SPOT Vegetation and MODIS, but were highly limited by the spatial resolution (1km and 250m respectively) of these sensors. The use of these sensors in vegetation classification is very valuable but fluvial landscapes of medium size rivers cannot effectively be characterized at this coarse resolution.

Alternative classifications using multispectral plus LiDAR data, or aerial photographs still has a classification error that leads to large uncertainties in flood modelling. Multitemporal spectral data at medium scale has proven its value in different applications, but it is not known whether it will work for patchy landscapes like the lowland floodplains of the Rhine distributaries. Seasonal variation and management allows vegetation to vary dynamically leading to a high spatiotemporal variation of vegetation structural characteristics including LAI and inherent roughness patterns. However ground based measurement of structural characteristics are limited in spatial coverage and the frequency of updates.

1.3. Research Objectives

The objective of this study is to use medium resolution multitemporal DMC satellite imagery to improve the classification of the IJssel floodplain vegetation from the current 69% accuracy achieved by Knotters *et al.*(In press). The long term goal is to provide efficient and effective tools for characterization of vegetation roughness coefficients in hydrodynamic flood modelling.

Specific sub-objectives

- ❑ to produce temporal NDVI profiles by landcover type using field reference data
- ❑ to classify landcover using hypertemporal NDVI profiles
- ❑ to predict Leaf Area Index (LAI) using hypertemporal DMC remote sensing products vis-à-vis field measurements

1.4. Research Questions

i. *With respect to hypertemporal image analysis, can DMC satellite images produce temporal NDVI profiles that are landcover specific?*
ii. *In reference to the first question, can hypertemporal NDVI profiles be used to accurately classify landcover?*
iii. *Can DMC hypertemporal images be used to accurately predict Leaf Area Index?*

1.5. Approach

The study entailed a reconnaissance of the area using ecotope maps and high resolution aerial photography of 2003 to identify suitable areas for fieldwork data collection. A purposive sampling strategy was designed to distribute sampling areas evenly over the floodplain to include all landcover types that have been identified using the ecotope maps and classes also identified by Knotters & Brus (In press). DMC International Imaging (Pty) Ltd supplied imagery exclusively for this study. The images shall be referred to as DMC Satellite images. The aim was to get a minimum of two cloud free scenes per month, to look at a two week interval landcover/landuse activity and associated phenological changes. The schematic in Figure 2 provides the approach used for this study.

1.6. Study area

The study area is the floodplain within the winter dyke along the river IJssel in the Netherlands. It stretches for approximately 40km from the City of Zwolle (N52 30 14, E06 02 45) to the city of Arnhem (N52 57 54, E05 57 10). The Ijssel is one of the three branches of the river Rhine which enters the Netherlands from Germany on the South East.

The study area, as corroborated by Straatsma (2007), is generally flat with elevation differences mostly less than 1 metre, except for a series of wind-blown ridges, which are approximately 4 metres higher than the rest of the floodplain. Land cover is a combination of arable land, meadows, open water and nature areas that partly consisted of forests. Arable land is mainly maize and haygrass making with typical plot size of 200mx200m. Forests comprise softwood forest (willow, (*Salix alba, Salix viminalis*), poplar (*Populus nigra, Populus x canadensis*)) and hardwood forest (oak (*Quercus robur*), ash (*Fraxinus excelsior*)) in various stages of development, and a small mature pine stand (*Pinus sylvestris*). The typical inundation depth of these floodplains is 3 metres, but water depths may rise to 5 metres in case of extreme flood events (Straatsma, 2007).

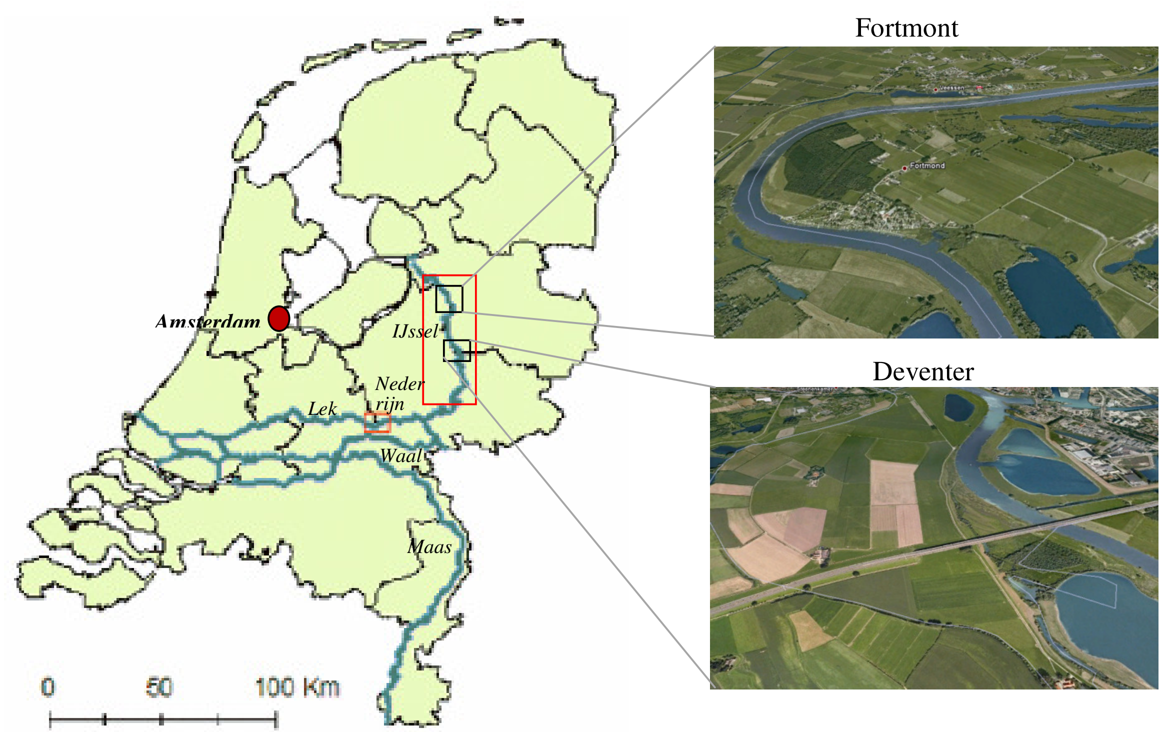

Figure 1 - Study area in the Netherlands. The landcover is characterised by forest patches, lake and river water, agricultural crop with occasional bare areas. (source: Addink *et al.* (2009) and Googleearth (2010))

2. Literature Review

2.1. Flood modelling

The Netherlands suffered a major flood event in 1995, the highest since 1926 (Silva *et al.*, 2001). It was after this flood that the government initiated a lot of water and flood management programmes that included expansion of flood discharge capacity. Further in 2006, the Dutch government adopted the Spatial Planning Key Decision *Room for the River*, aiming at reducing flood-water levels, together with restoring riverine ecosystems. To account for changes in floodplain vegetation over time, the government requires five-yearly updates of vegetation maps, to monitor hydraulic roughness patterns and ecological quality of the floodplain(Addink et al., 2009). This requirement initiated the need for robust models that could take advantage of latest developments in technology for extraction of floodplain variables for flood modeling parameterization.

The modeling of the water levels is bound with uncertainty due to the complexity of the input and the various schematizations of the interaction between the water, the river bed and floodplain vegetation. Much effort has gone into parameterizing the floodplain vegetation for flood modeling, but due to this uncertainty in floodplain vegetation classification and errors in the used LUTs , some arbitrary choices still have to be made (Straatsma and Baptist, 2008). In many model applications on vegetation roughness the drag coefficient is set to different values for submerged and emergent vegetation, which also involves an arbitrary choice (Straatsma and Baptist, 2008). This is done, for example, in an effort to account for rough vegetation surfaces or for the leaves on the branches. Shortcomings in the model scheme, computation method or model input can be compensated using roughness values that are physically not representative and lead to large uncertainty. The accuracy of the model input, calibration and sensitivity all influence the accuracy of the predicted peak water levels (Straatsma, 2007).

Some progress has been made in modelling flow around vegetative structures, however the difficulty of measuring vegetation biophysical properties, and their spatial and temporal variability, means that converting these results into a form suitable for 2-D hydraulic modelling still remain inaccurate (Horritt, 2006). According to Hesselink *et al.* (2003), sensitivity analyses on flood models show a large influence of floodplain topography and hydraulic friction caused by vegetation on the propagation of the inundation. The spatial and temporal variation in vegetation significantly influences flood hazard characteristics because of changes induced in hydraulic resistance throughout the floodplain

2.2. Vegetation characteristics

It has been generally agreed that vegetation increases flow resistance, changes backwater profiles, and modifies sediment transport and deposition (Yen, 2002). Vegetation in floodplains adds more complexity to flow structure and velocity of the flood wave (Huai Wen-xin *et al.*, 2008) . A number of vegetation properties like height, density, LAI, drag coefficient, plant spacing and orientation of rough patches have been tested in many models and their effects documented. For example test results on rigid vegetation showed that planting density and array model have enormous impact on flow velocity(Huai Wen-xin et al., 2008). Li and Zeng (2009) have also shown the importance of vegetation in the flow properties where decrease in vegetation density resulted in increased flow in the main channel and the floodplain. Järvelä (2004) studied the effect of leafy bushes or trees versus leafless bushes or trees on flow resistance and found that there was high significance of effect of leafed vegetation on flow resistance. Cotton *et al*. (2006) also showed that growth and die-back of in-stream macrophytes at the reach scale have a fundamental effect on the dynamics of flow.

The simplest and most practical way is to investigate the relationships between LAI and NDVI values is by means of regression models. Such relationships usually result in different mathematical forms with empirical coefficients that vary, depending primarily on vegetation type (Colombo *et al.*, 2003). However Fan *et al.* (2009) noted that LAI measurements are problematic for low stature vegetation including grasslands but stress the usefulness of NDVI as a direct estimator of LAI. The authors note that whenever possible LAI estimation using NDVI values is also suitable for low stature vegetation like grass because of the downward looking properties of the satellite sensors.

With field measured LAI corresponding to NDVI, backward regression analysis can be applied to determine LAI, from which the imagery can in turn be used to directly predict vegetation roughness coefficients in flood models (Jarvela, 2004). During the study, the author found that the major contributor to the drag of most trees is the drag of the leaves. And considering that LAI is the measure of leaf density then the leaf area index (LAI) is a key parameter in determining the density effects on coefficient of friction (f) caused by vegetation.

2.3. Mapping

To support the transition from traditional flood defence strategies to a flood risk management approach at the basin scale in Europe, the EU has adopted a new Directive (2007/60/EC) at the end of 2007. One of the major tasks which member states must carry out in order to comply with this Directive is to map flood hazards and risks in their territory (de Moel *et al*., 2009). Surveys of channel and floodplain characteristics and change have traditionally been conducted in the field (Wright et al., 2000). The drawback to these surveys is that they are local in extent, time consuming, relatively costly, and therefore, seldom carried out for more than a few years. As noted in section 1.1.1 , the Netherlands uses ecotope maps for parameterization of flood models and these maps are manually delineated. According to Knotters & Brus (In press) an ecotope is defined as a spatially bounded ecological unit, whose composition and development are determined by abiotic, biotic and anthropogenic aspects. Ecotopes are more or less homogeneous units at landscape scale, which are discernible from similarities and contrasts in geomorphology and hydrology, vegetation structure and land use. The authors further purport that ecotope maps are used as basic information for policy and management purposes, regarding water quantity, ecological system knowledge and restoration and development projects of the Dutch water systems. (Knotters and Brus, In press). It is evident that the accuracy behind the ecotope maps is highly desirable. But as Congalton & Green (1999) have already noted, a map accuracy depends on a great many factors, including the amount of effort, level of detail, classification scheme, and variability of classes being mapped.

Wright *et al.*(2000) used airplane-based digital imagery and GIS technology to classify and map hydrogeomorphic stream units in two alpine streams in and adjacent to Yellowstone National Park, USA. They used high resolution multispectral imagery with field maps and noted the difficulty in

proper georectification due to the disparities between the data sources and format. They achieved an overall accuracy of 80% using a method they called Alternative Joint Probability (AJP) where the pixels on the imagery were allowed to be assigned to multiple geomorphological units.
Remotely sensed digital imagery provides a potential means for observing and monitoring change in fluvial systems at reach scales across entire watersheds, while also providing a database for quantitative analysis that is potentially less costly on long-term basis.The latest advances in satellite technology provide both enhanced spatial and temporal methods that can enable fast, efficient and cost effective data acquisition and analysis for classification and mapping of floodplain vegetation.

2.4. Remote Sensing Methods

Over the years many different remote sensing techniques have been applied to vegetation classification with varying results. The most contributing factor is the different sensor properties and their combination in and with the classification methods. Zurita-Miller *et al.* (2009) have demonstrated the importance of balancing the temporal and spatial resolutions of sensors in studying vegetation dynamics. However to capture these aspects they had to downscale MERIS data with good temporal resolution (3days) but unsuitable spatial resolution (300m at full resolution, FR) to "Landsat like" properties with 30m spatial resolution but unsuitable temporal resolution (16days). The goal of this downscaling methodology by Zurita-Miller *et al.* (2009), was to take advantage of the best properties on either images and be able to reconstruct images with a high spatial and temporal fidelity while possessing the spectral properties to calculate vegetation indices. The accuracy of this method is limited by priori knowledge of the pixels with respect to scene composition and the number of components that can be unmixed is limited by the number of spectral bands of the image. The images need to be acquired at about the same date and co-registration of the images needs to be done perfectly as this alters either the geometric or the radiometric properties of the image.

Airbone Laser Scanning (ALS) has proven ability to quantitatively map vegetation structural characteristics such as forest vegetation height, biomass, basal area, leaf area index and vegetation density (Straatsma and Middelkoop, 2006). It has provided good results in vegetation characteristic classification, however during an experimental study by Straatsma & Baptist (2008) the distinction between meadows and herbaceous vegetation was still difficult. This is due to the fact that ALS data has noise level around 4 cm (Straatsma and Baptist, 2008), and therefore vegetation differentiation at this level is problematic. The other major challenge is ALS is still an expensive technology and this method is only suitable for static classification and not for trajectory monitoring of vegetation dynamics over the growing season.

In recent years there has been more developments and improvements in both spatial and temporal characteristics of satellite products and also to directly include characterization of vegetation by indices. This includes MODIS 4, CBERS, SPOT Vegetation and MERIS. Satellite imagery provides an opportunity to track these changes and parameterize the flood models accurately at any given point in time. Despite the enhanced spatial and spectral resolution of these sensors, an accurate characterization of heterogeneous and patchy floodplains with anthropogenic activities still requires a specific balance between the spectral, spatial and temporal characteristics which is hardly found in any one of the mentioned sensors.

According to Townsend and Walsh (2001) researchers have not adequately been able to discriminate and map relevant plant communities with sufficient floristic detail using satellite imagery. Satellite technology and remote sensing systems have traditionally been used to map broad landcover classes through 'flat' or one-dimensional classification schemes related to differences in physiognomy and dominant canopy species. In complex communities such as those found in floodplain landcover, satellite imagery has not been used adequately to make interpretations of community structure beyond broad ecological generalizations. Challenges have further emerged where researchers needed to correlate ground measurements to satellite products as satellite sensors generalize values over a relatively non homogenous landscape (de Bie *et al.*, 2008). Many models require landscape level parameterization but the trade-off between the spatial and temporal resolution provided by many sensors is huge.

2.5. Image Classification

According to Richards and Jia (2006), identification of features in remote sensing imagery by photo interpretation is effective at global scale, only when a few pixels are involved or the number of spectral bands is limited to three. When these levels are exceeded detailed procedures and algorithms must be used for automated and quantitative classification. In a classification, labels are attached to pixels in view of their spectral character. There are two broad categories of classification; unsupervised and supervised classification. In unsupervised classification pixels in an image are assigned to spectral classes without user having fore knowledge of names of the classes while in supervised classification the spectral classes in the image are known and grouped by the use of a training set. Supervised classification is more complex in its operation and depends on whether they are statistical or non-statistical. In some instances these categories are combined into a hybrid methodology (Richards and Jia, 2006).

Many methods exist in classification of floodplain vegetation. In determining plant community composition and structure in south eastern USA, Townsend & Walsh (2001) used Landsat TM at 30m resolution but experienced difficulties with selection of images due to the lower temporal properties. The images suffered overlap with flood events and could not accurately characterize succession activities where recent harvesting may have occurred. However they report an overall accuracy of 92% with the use of hierarchical classification method, where ISODATA clustering is applied first then the image is segmented according to the level of the required grouping. The use of the temporal dimension and NDVI values as an index for ecosystem functioning provides an untapped stratification tool for mapping and monitoring. De Bie *et al.* (2008) used temporal profiles of SPOT Vegetation for crop mapping and change detection in West Iberia and picked the sensor's 1km resolution as the downside.

Addink et al. (2009) developed a method which combines object-based analysis of Colour InfraRed aerial photographs with knowledge on vegetation succession paths. The authors claim that object-based classification produces more accurate results, because the studied objects represent vegetation patches at the surface better. They achieved an overall classification accuracy of 56%. Object oriented classification is based on fuzzy logic, to allow the integration of a broad spectrum of different object features such as spectral values, shape or texture for classification.

2.5.1. Spectral Angle Mapper (SAM)

Spectral Angle Mapper (SAM) is a physically-based spectral classification that uses an *n*-D angle to match pixels to reference spectra. The algorithm determines the spectral similarity between two spectra by calculating the angle between the spectra and treating them as vectors in a space with dimensionality equal to the number of bands (Kruse *et al*., 1993). According to the authors, this technique, when used on calibrated reflectance data, is relatively insensitive to illumination and albedo effects. SAM is suitable for hyperspectral data as standard classification procedures often fail to obtain reliable class definition with data of high dimensionality (Richards and Jia, 2006).

2.5.2. Maximum Likelihood Classification (MLC)

This is the most common classification method used with remote sensing data. Maximum likelihood classification assumes that the statistics for each class in each band are normally distributed and calculates the probability that a given pixel belongs to a specific class (Richards and Jia, 2006).
In a test study to classify tropical forest with airborne hyperspectral data, MLC outperformed, Artificial Neural Networks (ANN), Decision Tree (DT) and even SAM at 86%, 84%, 51% and 49% respectively (Shafri *et al*., 2007).

2.5.3. NDVI Profile Classification

According to Richards & Jia (2006) classification cost (processing and number of classes) increases with the number of features used to describe a pixel, that is the number of spectral bands. They further note that for maximum likelihood classification this increase is quadratic. For the NDVI image stack to be classified, the number of features is the number of temporal pixel stacks used to describe any pixel at any particular location. Therefore NDVI Profile Classification uses the temporal dimension out of the image stack to classify an image. This method can be looked at to what Richards and Jia (2006) refer to as hybrid methodology. An unsupervised classification, ISODATA, is used as a prerequisite to profile matching. The ISODATA clustering method uses spectral distance, as in the sequential method. It iteratively classifies the pixels, redefines the criteria for each class, and classifies again, so that the spectral distance patterns in the data gradually emerge (Khan *et al.*, In press). Once ISODATA has been performed, NDVI profiles are produced from the ISODATA clusters and regrouped taking the temporal dimension into consideration. The set back with this method is that its techniques have not matured and depends on the researchers intuition for accurate classification. The classification is not as objective as it would be if it was algorithm based. Verbal communication with de Bie (2010) is that while there are advances in this field, the methods are still limited in terms of algorithms that can take advantage of the complex temporally influenced shapes. Many researchers still depend on visual interpretation.

Geerken (2009) has looked at existing methods in algorithm based NDVI profile classification and asserts that a number of them only focus on conventional interpretations of some NDVI variable like NDVImax or accumulated NDVI. The author argues that even though these methods have tried to exploit the information contained in the shape of the profile, they have not fully utilised the temporal aspects of the shape itself. The author proposed a shape classifier method based on the Fourier components magnitude and phase and claims that this method can differentiate and classify landcover types, vegetation types, crops or crop management techniques. However Evans & Geerken (2006) admit that this method despite having been developed and well suited for analysing time series, it has not really been developed to carry out vegetation classification using NDVI data series. Geerken (2009) used this method on SPOT Vegetation with 10day interval composite and MODIS with 16day interval composite. However this methodology also depends on the data quality, the number of time steps defined by the compositing interval, and the temporal variations of phonological features to be detected (Geerken, 2009). It further requires that reference cycles to be established on which further classification will be based and these reference cycles should be derived from either expert opinion, field data or image characteristics.

2.6. Leaf Area Index & NDVI

The normalized difference vegetation index (NDVI) has been extensively used for vegetation monitoring. At global and regional scales, NDVI is typically computed from the data provided by the Advanced Very High Resolution Radiometer (AVHRR) onboard National Oceanic and Atmospheric Administration (NOAA) satellites. However, the AVHRR sensor was designed for meteorological applications and its radiometric and spectral performances are, therefore, not optimal for monitoring canopies (Zurita-Milla *et al.*, 2009).

To investigate the relationship between NDVI and LAI, field based measurements of LAI are necessary. The traditional method of estimating LAI is to harvest vegetation in a certain area and measure all the one-sided leaf areas directly(Fan et al., 2009). The method is time consuming and destructive. Other non destructive and rapid methods are available for estimation of LAI and the LAI-2000 is one of the tools that provide that functionality. The LAI-2000 (Li-COR, 1992) measures light interception in five zenith angles simultaneously, through a fish-eye light sensor. The disadvantage of this indirect method is that in some cases it can underestimate the value of LAI in very dense canopies from 25% to 50%, as it does not account for leaves that lay on each other, and essentially act as one leaf according to the theoretical LAI models (Breda, 2003). This instrument is very easy to apply during the field research, however its spatial range is limited because of the large spatial heterogeneity of floodplain vegetation structures (Szoszkiewicz *et al*., 2003).

Relationship between LAI and NDVI is specific to both vegetation physical properties and location characteristics. Fan *et al.* (2009) had to use a global model with leaf dry matter (LDM) of the area of interest that was developed in previous studies to access the required relation coefficients. However, the main disadvantages of the NDVI are the inherent nonlinearity of ratio-based indices, scaling problems, saturated signals over high biomass conditions, and its high sensitivity to canopy background variations (Huete *et al.*, 2002). Further error sources include cloud contamination and insufficient atmospheric transfer corrections for atmospheric aerosols, gases, and water vapour and bidirectional reflectance. All these effects result in a decrease of the observed NDVI. To eliminate or reduce the impact of these effects, researchers use compositing methods that usually take the maximum NDVI value over images of some predetermined time interval. Titterbrans *et al.* (2009) and De Bie, *et al.* (2008) used a 16day composite for MODIS. However the method using NDVI to estimate LAI has a limitation in its applicability at the higher ranges of LAI, for NDVI saturates when the vegetation canopy tends to be closed and in this case NDVI can no longer be used to detect any differences in LAI (Pontailler *et al.*, 2003). The difficulty to relate LAI to NDVI has been experienced by other researchers as well, the relation between the NDVI and forest LAI has been shown to fail when canopy cover is low and there is spatial variation in understory reflectance (Danson and Plummer, 1995).

The LAI measurements can also be related directly to the friction coefficient like the Weisbach ***f*** using the equation (1) as derived by Järvelä (2004).

$$f = 4C_{dx}LAI\left(\frac{U}{U_x}\right)^x \tag{1}$$

where f is the vegetation friction coefficient

C_{dx}	=	species specific vegetal drag coefficient
LAI	=	Leaf Area Index
X	=	a parameter unique to vegetation type
U_x	=	The lowest flow velocity for determining parameter

3. Materials and Methods

3.1. Flow diagram

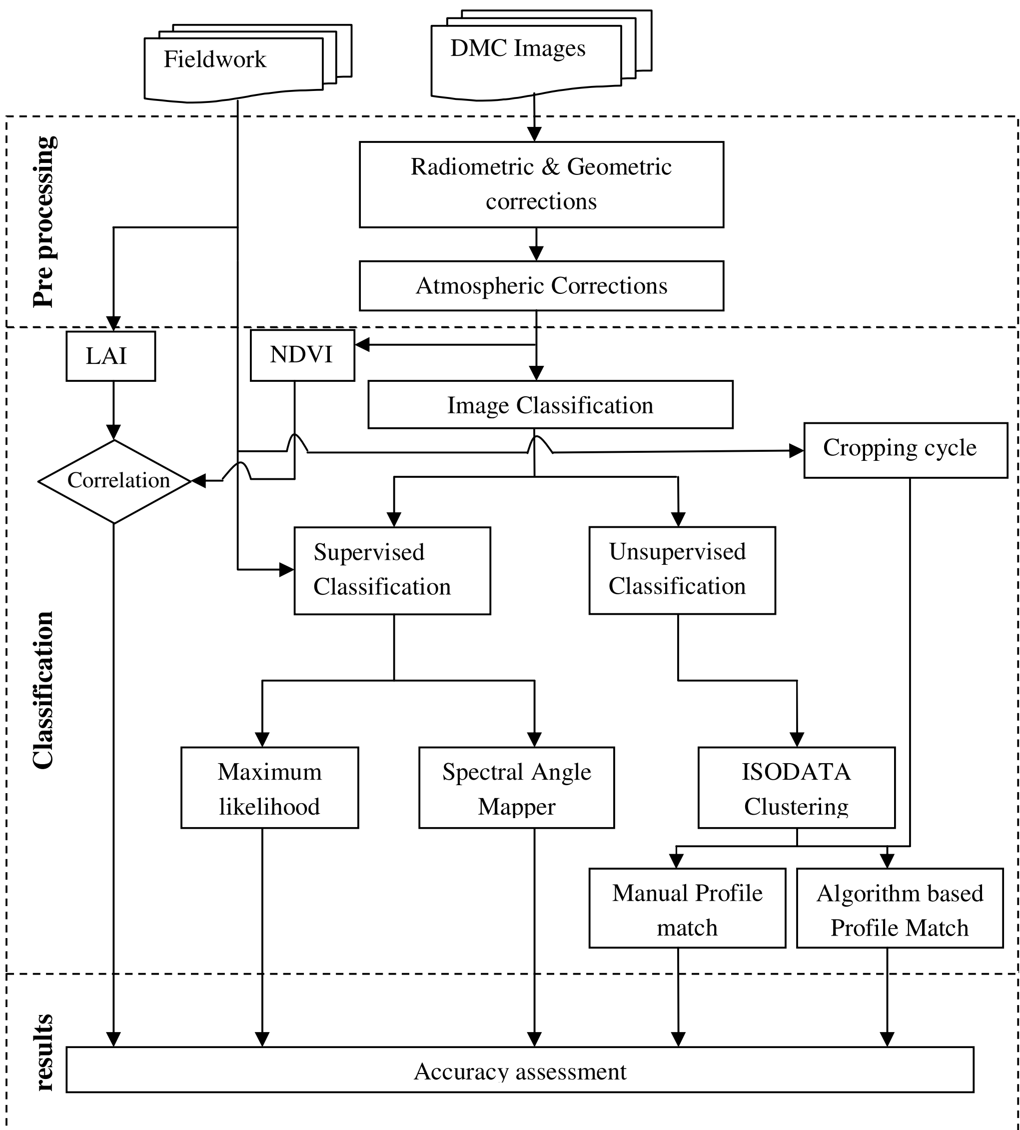

Figure 2 - Conceptual flow diagram

3.2. Materials

3.2.1. Images

Images used for this research were supplied by DMCii International (Pty) Ltd, UK for research purposes. DMCii supplies images in Geotiff format and in three different product levels, L0R, L1R and L1T;

- L0R - raw satellite data split into the 3 spectral bands (NIR, Red and Green) with a radiometric correction applied to all bands
- L1R – the 3 spectral bands from L0R product are co-registered and delivered as one product
- L1T - Orthorectified product derived from the L1R product using manually collected GCPs from Landsat ETM+ data and SRTM DEM V31 data

Only L1R and L1T products were used in this study. The L1T products were used as is while the L1R products were georeferenced (see Georeferencing and clipping section). The DMC sensor properties are listed below:

Sensor type	*DMC SLIM 6*
Spatial Resolution	*32metres*
Temporal Resolution	*daily (constellation)*
Bands	*3 (NIR, Red, Green) + Pan*
Swath width	*324 km*
Scanner type	*Whiskbroom*
IFoV	*26.62^{o}*

The aim was to select a minimum of two images per month with a spacing of two weeks between the images over the 2009 growing season. The Netherlands growing season runs from April to October over a span of seven months but during this time it was difficult to acquire the images as was the initial interest. The 32 supplied images were not exactly in the required spacing and of which three images could not be used because they missed gain and offset values. The gain and offset values were needed to rescale the images from the supply DN values to radiance values as per equation (2). Eight images had cloud or haze artefacts prominent in many parts of the image while two images had part of the study area cut. The most interference was caused by haze which was less prominent in the thumbnails used for image selection but was evident after supply of the images. See (Figure 3) for the list and dates of images used.

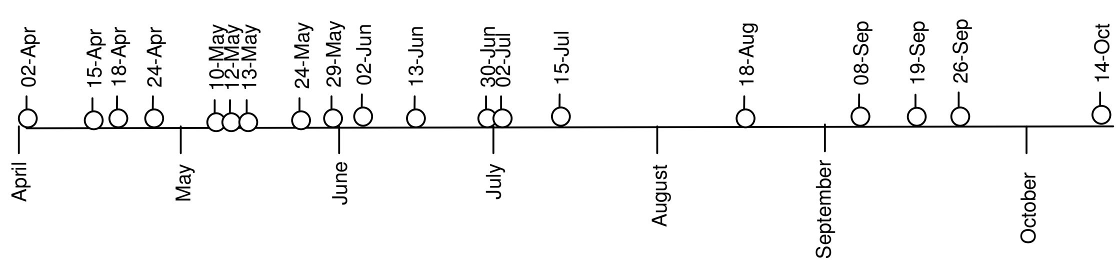

Figure 3 – The good images that remained over the 7month growth period. The period between July 15th and August 18th was missed because of problems mentioned above.

3.2.2. Ecotope Maps

Ecotope maps were used for area reconnaissance as a precondition prior to fieldwork. The ecotope maps were regrouped into eight distinctive classes describing the landcover types of interest (see Figure 4). The classification of ecotope map takes into account properties associated with its specific location of the landcover units.

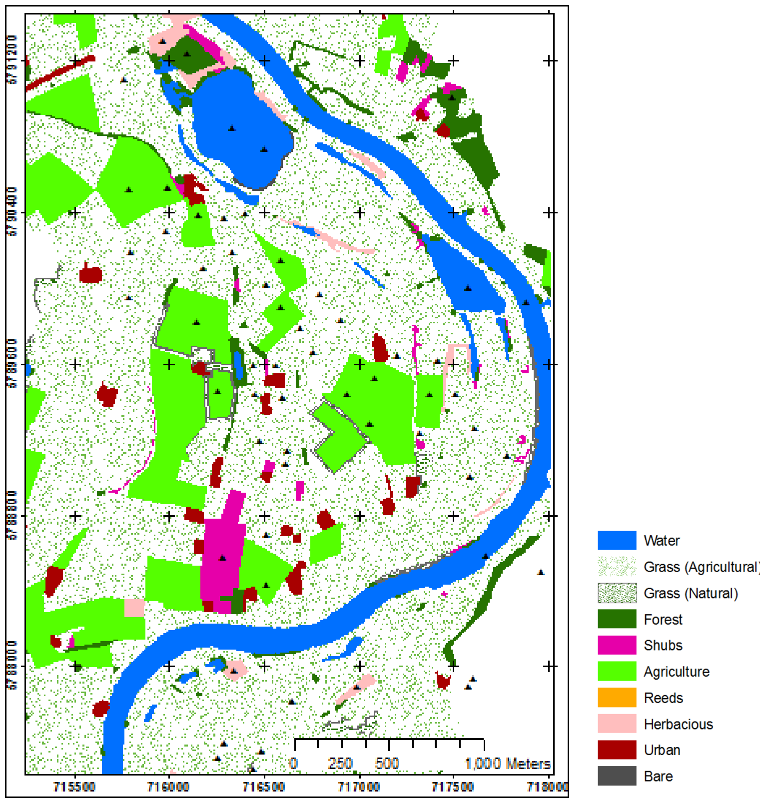

Figure 4- Re-grouped ecotope map with overlay of field sample points

3.2.3. Field work

In order to assess the accuracy of the classification, field reference data was collected. A purposive sampling strategy was used where sampling locations were predetermined to be at specific landcover of interest. It was also predetermined that sampling would be done on plots that covered dimensions of minimum 90mx90m in line with requirements as discussed in section (3.2.4). Sampling areas were located at Fortmond and the area south of Deventer and north of Zutphen, see (Figure 5). These areas were wider parts of the floodplain and contained most of the landcover types of interest. The sampling strategy is non-probability in that any field measurement has a fair chance of being included in the sample population. The researcher made sure that the landcover classes that were predetermined were sampled the required number of times. The method was suitable because the landcover to be investigated was already known in terms of its structure and diversity from the reconnaissance maps. The landcover types were grouped into forest, water, herb, shrub, grass, agriculture, urban and bare in reference to classes established by Knotters and Brus (in press). The aim was to sample each landcover type a minimum of 15 points but some landcover types like bare and shrub were not in abundance. A lot of shrub and herbaceous areas did not cover the required dimensions of the plot.

Since the satellite imagery used with the fieldwork data was 32m resolution, the landcover areas that were selected for sampling were those with dimensions of at least 90x90m. This follows the methodology used by Townsend & Walsh (2001) that the minimum dimensions of a sample area, *A*, should be estimated as: $A = P(1+2L)$, where *P* is the pixel dimension, and *L* is the accuracy of location in terms of numbers of pixels. This ensured a minimum of one cell positional error in all directions of the image. The field points were collected within landcover plots that were also generally homogeneous such that the cell value is more or less representative of the landcover within the 90mx90 pixel dimensions. A total of 186 field samples were collected.

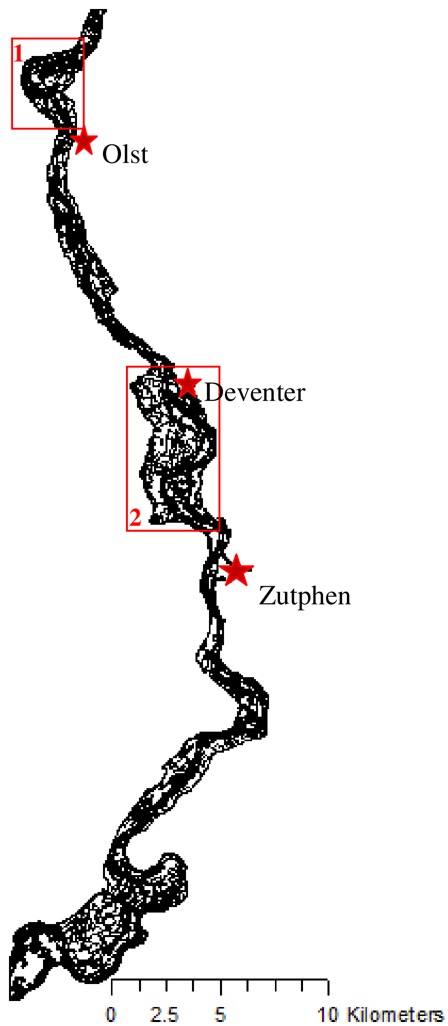

Figure 5 - Floodplain of the IJssel river with sampling locations.

3.2.4. LAI Measurements

To evaluate whether field measured LAI for this particular area will be correlated with the satellite imagery used for this study, LAI measurements were collected for each landcover with a vegetation height of greater than 30cm. Despite the claim by Li-Cor that the instrument can be used for virtually any canopy height, it was very difficult to record LAI measurements for canopy cover that was less than 30cm. For any canopy cover that was less than this threshold the results were unreliable. The results of the LAI measurements are given on Appendix 5. The LAI measurements were plotted against NDVI values of known locations from the field data.

3.2.5. Questionnaire

For the landcover type that was agriculture, a questionnaire was distributed to the farmers, see appendix 2. The activities associated with the landcover under observation were recorded in response to the questionnaire by the farmers. The farmers were asked about their farming activities including types of crop and times of cropping. Twelve farmers were interviewed and each farmer's response was related to more than one field. A history of 28 farms was recorded.

3.3. Image Processing

3.3.1. Georeferencing and clipping

The L1R products were georeferenced using image to image geometric correction without the use of a DEM. This is because the study area, as discussed in section 1.6, is relatively flat and therefore effects of terrain on geometric correction can be ignored. The images were corrected at precision better than 0.5 pixels root mean square error (RMSe). According to Khorram *et al.* (1999) an RMSe of more than 0.5pixels may result in the identification of spurious areas of change among the datasets, caused by the erroneous difference in the location of the cells being compared. Polynomial with nearest neighbour (NN) was used. This method resamples the cell values but ensures that the resampled values were as close to the original pixel value as possible while compensating for rotation, scale, skewness, and offset adjustment. The method preserves the radiometric and spectral information in the imagery (Richards and Jia, 2006)

3.3.2. Radiometric Correction

Pre-processing of multitemporal data is essential to help minimise effects that obscure links between the image data and the biophysical phenomena being studied (Paolini *et al.*, 2006) . The objective is to remove errors associated with data acquisition including sensor effects, atmospheric and illumination effects and mis-registration. Paolini *et al.* (2006) corroborates that pre-processing for change detection is more demanding than single-image cases due to the need to make equitable comparisons. The goal of radiometric correction is to remove or compensate for effects that cause variation in radiance of a target object so that only actual changes in ground target remain. The resulting radiance values are used to calculate surface reflectance that simulate data acquisition under similar conditions but at different times steps (Du *et al.*, 2002).

To compensate for changing sensor sensitivity, the satellite data vendor recommended applying gain and bias values to rescale the image DNs. The gain and bias are used to convert the DNs back to true radiance (Crowley, 2008). All the images were rescaled using equation (2) below as provided in the DMC product manual. The scaling coefficients (gain and bias) are unique for every image and band and can be found in the metadata files that accompany every L1R and L1T product.

$$radiance = \frac{DN}{gain} + bias \qquad (2)$$

The unit of radiance is Watts per square metre steradian micrometre ($Wm^{-2}sr^{-1}\mu m^{-1}$)

Where : *radiance* = spectral radiance at the sensor's aperture
DN = digital number, quantity of solar radiance in a given wavelength band reflected from the ground
gain = a sensor adjusted factor to avoid unnecessary pixel saturation ($Wm^{-2}sr^{-1}\mu m^{-1}$)
bias = component to compensate for shifts caused by atmospheric scattering that add to the actual radiation reflected from the ground ($Wm^{-2}sr^{-1}\mu m^{-1}$)

3.3.3. Radiometric and Atmospheric correction

The goal of radiometric correction is to remove or compensate for effects that cause variation in radiance of a target except for actual changes in ground target itself to retrieve surface reflectances (absolute correction) or to normalize the digital counts obtained under the different conditions to be on a common scale (relative correction) (Du et al., 2002).

ATCOR model of ERDAS Imagine was tried but failed to run the DMC images. The model is an algorithm bundle that would have taken care of both absolute radiometric and atmospheric correction. Details of some of the encountered errors are discussed in section (5). Therefore Top of the Atmosphere (TOA) reflectance was calculated for one image selected at the middle of the growing season and closest to the time of fieldwork. The image was also selected to have very little or no atmospheric artefacts. The formula (2) used for TOA calculation for this image is was suggested by (Crowley, 2008), in the DMC product manual.

$$\rho_\lambda = \frac{\pi d^2 L_\lambda}{E_{0\lambda}\, cos\theta_s} \qquad (3)$$

Where ρ_λ = top of the atmosphere reflectance for band λ
$E_{0\lambda}$ = exoatmospheric solar irradiance band λ [$Wm^{-2}sr^{-1}\mu m^{-1}$]
θ_s = solar zenith angle at time of image capture in degrees [^{o}]
L_λ = Radiance in spectral band λ [$Wm^{-2}sr^{-1}\mu m^{-1}$]
d = earth-sun distance in Astronomical Units [AU]

The exo-atmospheric solar irradiance values and earth sun distance were accessed from the NASA (2010) website http://www.nasa.gov/ using the specific image dates to calculate the earth sun distance. The TOA equation does not take into account atmospheric effects (Crowley, 2008), but the resulting images can then be used for a comparative study.

The TOA reflectance from this image was used as the reference image to normalise the rest of the images. This is relative radiometric correction and normalises images using landscape elements (pixels) whose reflectance values are nearly constant over time (Paolini et al., 2006). This procedure assumes that pixels sampled at time 2 are linearly related to the pixels, at the same location, sampled at time 1, describing what is termed Pseudo Invariant Features (PIF). The PIF selection uses principal components analysis (PCA) as a more methodological approach to PIF selection. The PCA gives components on an image vector space whose correlation can be measured through the variance measure from the principal axis. According to Paolini *et al.* (2006), the method is relatively simple, accurate, requires less image interpretation and offers statistical objectivity on the selection of the PIFs.

This method was outlined by Du *et al.* (2002) and refined by Paolini *et al.* (2006) and explained in a step-by-step process by Galiatsatos *et al.* (Unpublished). Three images were selected, one at the beginning of the growing season (DC000a92p_L1T – April 15th), another around the middle of the growing season (DN000837t_L1T – July 2nd) and the third one around the end of the growing season (DU000fb6t_L1T – October 14th). With this distributed choice of images, it was assumed that pixels that showed non changing spectral characteristics on all images were ground objects that actually had little or no change over time in terms of reflectance.

The images were rearranged to multitemporal per band files and restacked respectively (see Figure 6) to produce three image stacks each with same bands from the original images. The non-standardised (variance-covariance matrix) PCA was run on each stack that comprised similar bands from the three images. PCA-1s from the three band stacks (see Figure 7) were classified using ISODATA clustering. The results were classified PCA outputs with class 1 containing minimal variability.

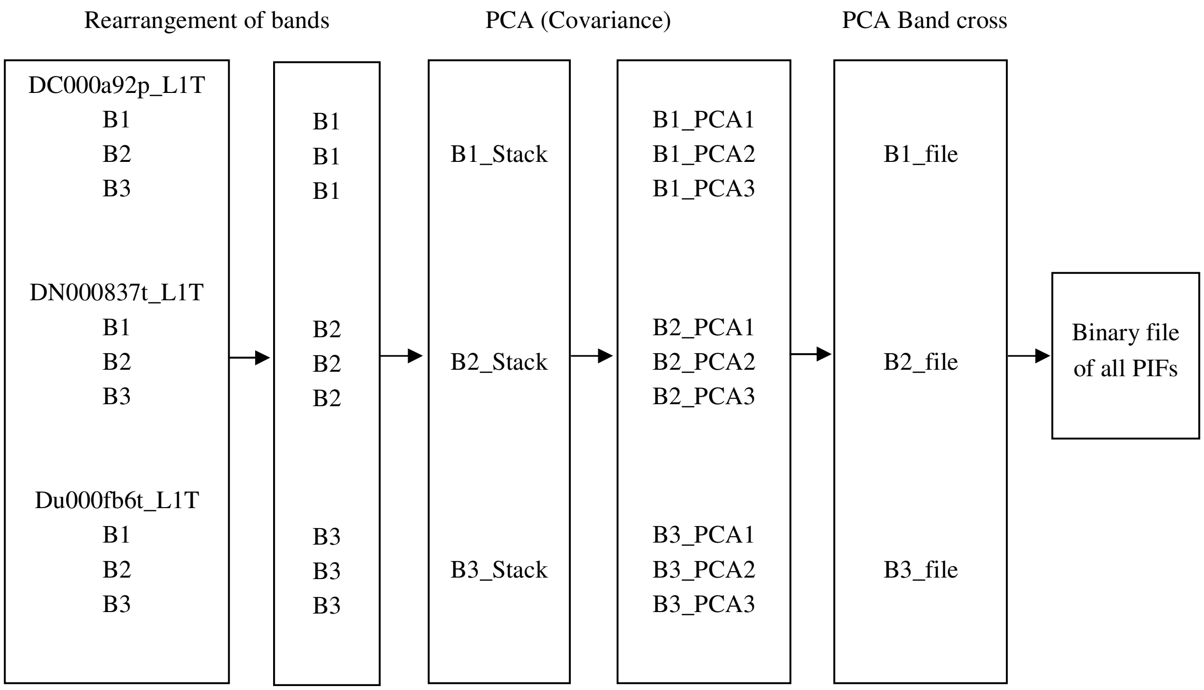

Figure 6 - PIF identification process adopted from Galiatsatos *et al.* (Unpublished)

Paolini *et al.* (2006) used Eigen values to set the threshold of how far from the principal axis would component values be accepted. This method was too detailed in terms of determining the threshold value so it was decided to accept the first class of the PCA output as the class that contained features that have little or no change in each band. The effect of this arbitrary choice is the areas considered as containing PIFs may be more or less than if the threshold value was used and that the threshold values may not correspond with the first class of each band combination.

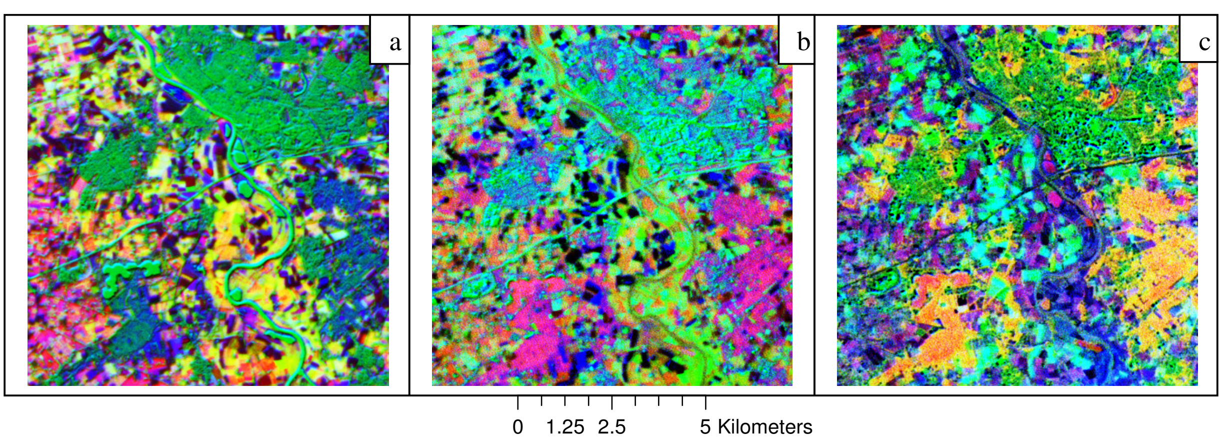

Figure 7 – RGB images of areas of no change in all the band1 (a), band 2 (b) and band 3 (c) are in green. Colours range from green – areas of no change to deep purple and red – areas with highest change.

The PCA output was converted into a binary image with class1 of each band assigned value of 1 and the rest of the classes assigned value of zero to create a transparent image except for the location of the PIFs, see Figure 8. The binary images of the three bands groups were crossed to create the final single binary image file which contained common PIF areas between the three bands.

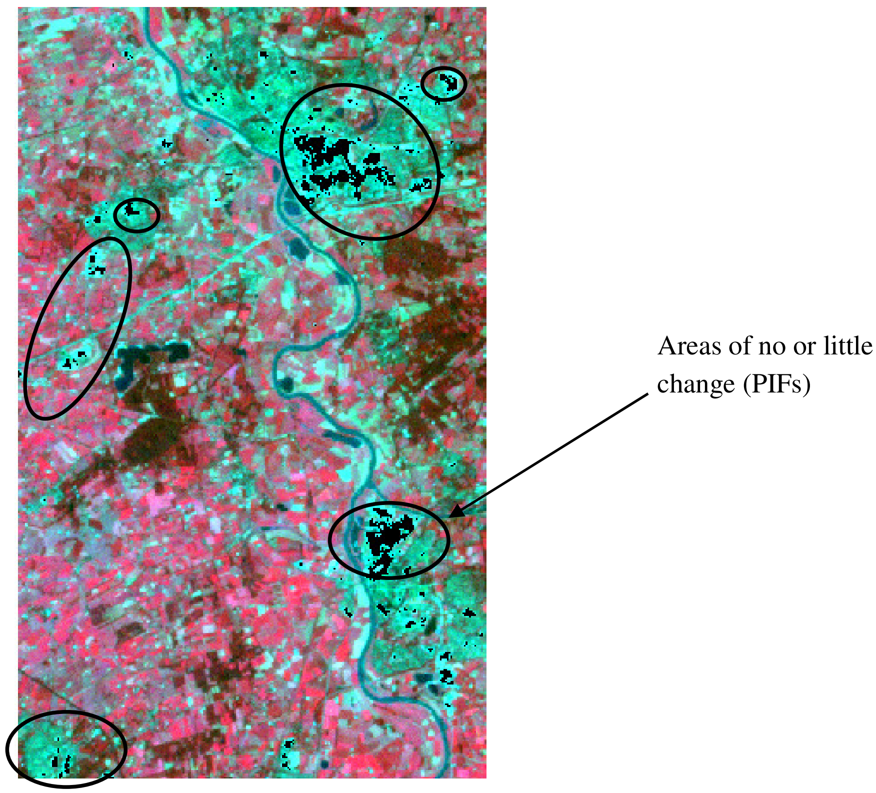

Figure 8 – Overlay of PIFs final binary image (black) over a false colour composite image.

3.3.4. Normalising Coefficients

This final binary image was used to extract DN values of the PIFs in each one of the images to be normalised and for each band. The values were used to produce scatter plots (see Figure 9) of TOA reflectance values of PIFs for the reference image against radiance values for PIFs of each band for each image to be normalised.

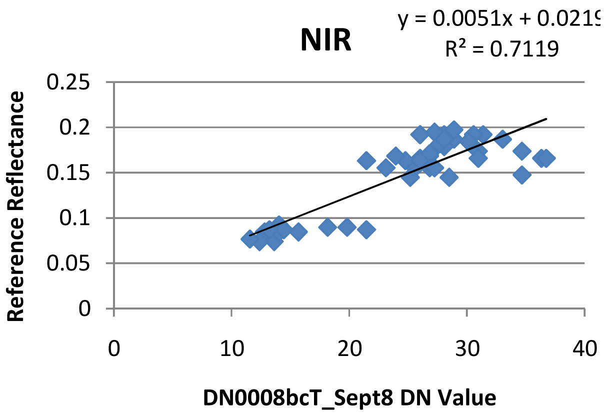

(a)

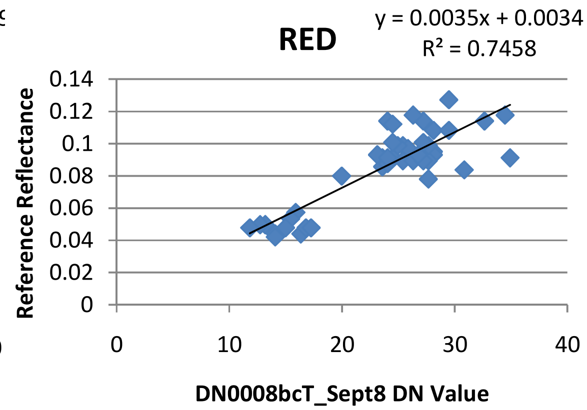

(b)

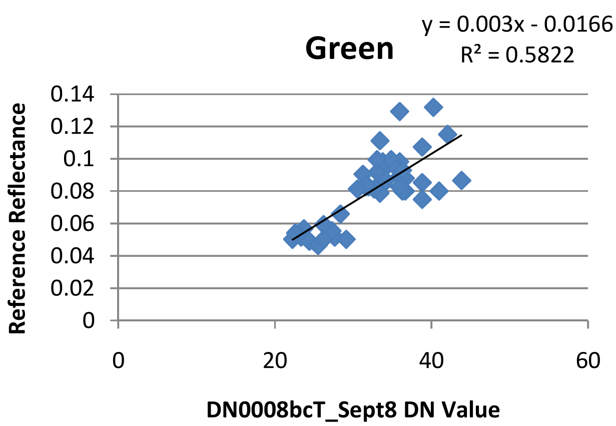

(c)

Figure 9 - Scatter plots of reflectance against radiance for the PIFs of reference reflectance against subject images radiance for NIR (a), Red (b) and Green (c). This process was repeated for all the 18images.

The resulting slope and offset from the scatter plots were used to convert each image band from radiance values to reflectance values using the regression equation (4) below. This slope and offset were the gain and bias coefficients that described the transformation from radiance to TOA reflectance equivalent for each subject image.

$$y = mx + c \tag{4}$$

Where: y = normalised image,
x = original image to be normalised,
m = the slope or gain for the image to rescale and
c = the offset/bias for the image to rescale.

After the images were transformed to TOA reflectance equivalent values, the results were used to calculate NDVI for each image using the NIR and RED bands as illustrated in equation (5) & (6).

$$NDVI = \frac{NIR-RED}{NIR+RED} \tag{5}$$

For the DMC images, the NIR band is band 1 (770nm – 900nm) while the red band is band 2 (620 – 700). Therefore the equation translates to

$$NDVI = \frac{band1-band2}{band1+band2} \tag{6}$$

An NDVI image stack was created from the resulting 19 layers.

3.4. Image Classification and Accuracy Assessment

An image stack of normalised images and another of the NDVI images were created. The two 19 layer stacks were used for images classification, SAM and MLC on the normalised image stacks and NDVI Profile Classification on the NDVI stack. The NDVI Profile classification has been explored by de Bie, *et al.* (2008) where a multivariate change detection method processes the full dimensionality of the multilayer image.

3.4.1. Spectral Angle Mapper (SAM)

Representative pixels of each of the classes were picked from the image to create a training set (end members) from the fieldwork data. The fieldwork data described the landcover as was observed at the time of fieldwork. The training set provided region of interest (ROI) as an average sprectra that was used as the reference spectra for the classification. SAM treats this dataset as having 57 spectral layers (3bands x19layers). Once the classification was run an accuracy assessment was run. The accuracy assessment used 186 fieldwork points, which excluded sugarbeet (*Beta vulgaris* L.) locations that could have been classified as either herb or agriculture.

3.4.2. Maximum Likelihood Classifier (MLC)

The ML classification was run with the training set created with the field work data. These were the spectral signatures that were collected in the areas that had the landcover that was known from the field work date. Histograms of the training set were displayed to evaluate the separability or the level of overlap between the classes. Again once the classification on the image stack was run, an accuracy assessment was performed using 186 of the field work points.

3.4.3. NDVI Profile Classification

The profile classification was performed on the NDVI stack. The number of classes used to run the unsupervised classification was determined using the Divergence statistics as used on similar work by de Bie *et al.*(2008) and Khan *et al.* (In press). This The Divergence statistics among others; the Euclidean, the Jeffries-Matusita (JM), Transformed Divergence, is one of the measures to quantify how separable various spectral classes are within a dataset. It was chosen for its comparatively ease on the computational cost (Richards and Jia, 2006).

ISODATA clustering was run on the NDVI image stack. The stack was classified into 10, 15, 20, 25,…., 90, 95, 100 classes and saving associated signature files. The number of iterations was limited to 50 and convergence threshold set to 1 for each of the runs. As a general rule of thumb, the number iterations is recommended to be half of the number of classes desired (de Bie and Toxopeus, unpublished), therefore since the largest number of classes required is 100, fifty was kept for all the class numbers such that this number is constant for all the runs.

For all the classification runs, minimum and average divergence values were collected from the associated signature file and displayed against the number of classes in a scatter plot in excel. It was realised that there was a clear and sudden deflection in the curve and values 50 and 65 respectively. Further classes, 63 and 67 were added to aid in the smoothing of the deflection. While the highest peak was at number of classed 65, the separability value went to an impractically huge number, (2,147,483,648). Therefore fifty classes were picked as the optimum number of classes because the peak had a definite value that was within a practical scale with the rest of the other values.

The fifty classes separability and its signatures were therefore selected to be the best optimal class separability and considered for NDVI calculation and classification. NDVI mean was extracted to excel from the statistics column for each of the 50 classes in the classification.
The NDVI values were plotted in Excel and produced a graph that showed the progression of mean NDVI over time. This produced a “spaghetti” graph on Figure 16.

The “spaghetti” graph was visually analysed to see which temporal class profiles looked similar, followed the same representative pattern and whether they could be merged under the same class. The general shape of the graphs was observed as well as specific behaviour at certain time locations. The fieldwork data was overlaid on the graph to see if there were any particular deflections in the graph that corresponded with field data. The ISODATA clustered images are also presented to see the effect of the 50 class clustering on the image categorization.

4. Results

4.1. Fieldwork

Figure 10 shows and overlay of sampling locations on ecotope maps while Figure 11 and 12 are temporal profiles of grass and maize respectively with an overlay of farming activity points extracted from field data.

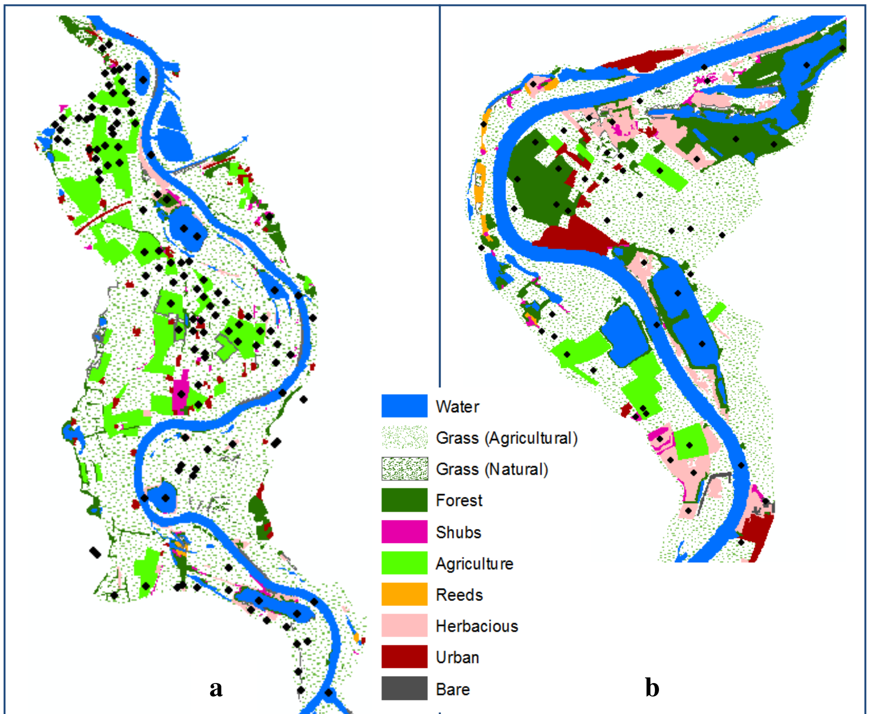

Figure 10 Sampling areas between Deventer and Zutphen (a) and in Fortmond (b)

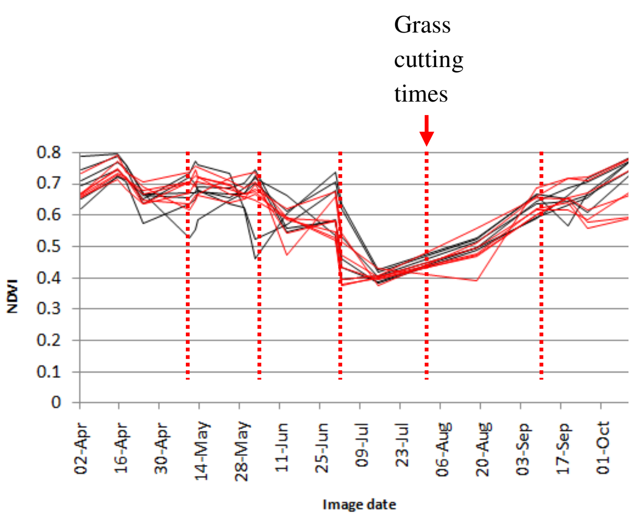

Figure 12 - NDVI temporal profile of grass. Grass include both for haymaking (black) and for meadow (red).

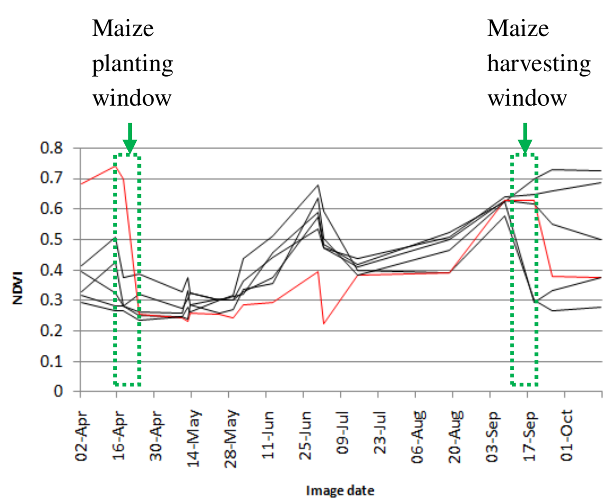

Figure 11 - NDVI temporal profile of Agriculture (Maize)

4.2. Image Classification

4.2.1. Spectral Angle mapper

The results of SAM classification showed an overall accuracy of 50.54% with the use of confusion matrix. The Kappa statistic is 0.4140. As shown on Figure 13 and Table 2. As can be observed SAM classification could not differentiate between water and urban.

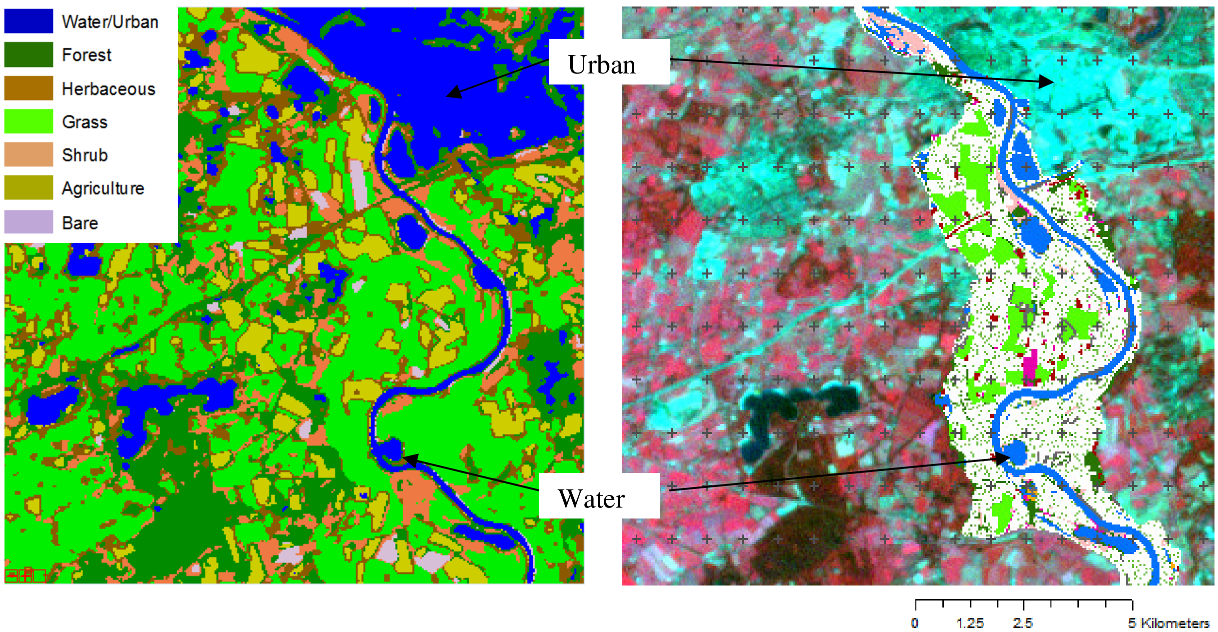

Figure 13 - Spectral Angle Mapper classifier shows a great overlap between many classes, e.g. water and urban.

	water	Forest	River	Shrub	Grass	Urban	Bare	Maize	Herb	Row Tota	Producers Accuracy	Users Accuracy
Water	10	0	1	0	0	0	0	0	0	11	100.00%	90.91%
Forest	0	7	0	1	0	0	0	0	0	8	70.00%	87.50%
River	0	0	8	0	0	0	0	0	1	9	88.89%	88.89%
Shrub	0	1	0	11	33	2	4	3	6	60	84.62%	18.33%
Grass	0	1	0	0	29	0	1	7	6	44	38.16%	65.91%
Urban	0	1	0	1	0	7	0	0	2	11	70.00%	63.64%
Bare	0	0	0	0	1	1	5	1	1	9	41.67%	55.56%
Maize	0	0	0	0	0	0	0	11	1	12	47.83%	91.67%
Herb	0	0	0	0	13	0	2	1	6	22	26.09%	27.27%
Column Total	10	10	9	13	76	10	12	23	23	186		

Overall Classification Accuracy = **50.54%**
Overall Kappa Statistics = **0.4140**

Table 1 – Confusion matrix of Spectral Angle Mapper classification.

4.2.2. Maximum Likelihood Classification (MLC)

MLC produced 54.54% accuracy. What is evident between MLC and SAM is that urban areas are well classified from water in MLC than in SAM (Figure 14). The error matrix is presented in Table 3.

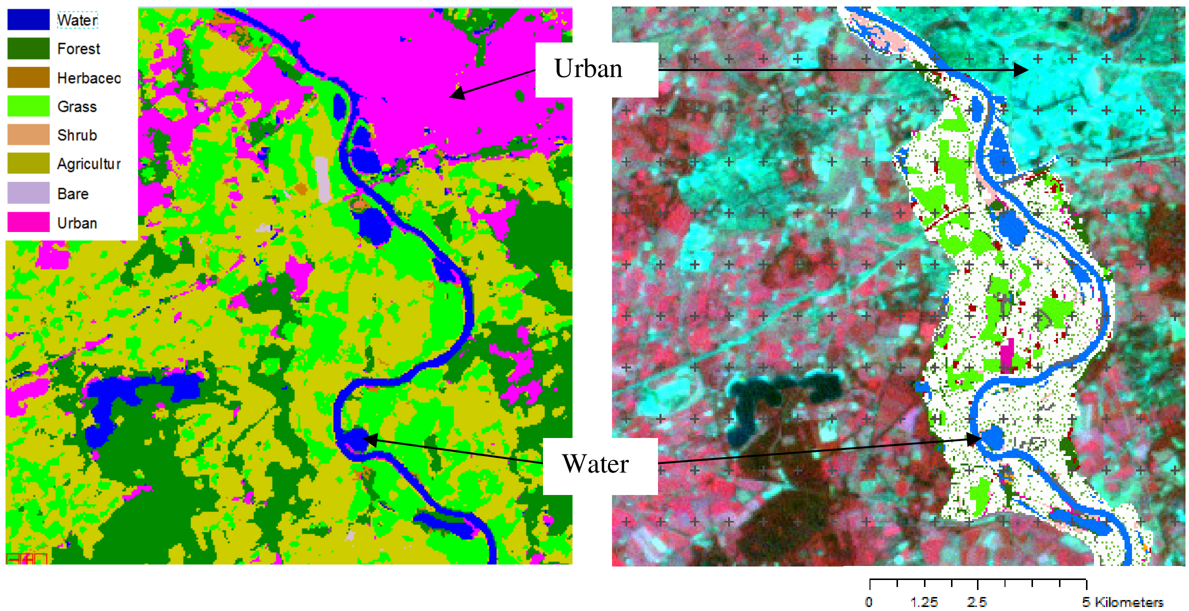

Figure 14 - Maximum Likelihood Classifier

	Wat	For	Rv	Gr	Ma	Shr	Her	Bar	Urb	Row total	Producers Accuracy ---------	Users Accuracy -----
Water	19	0	0	0	0	0	0	0	0	19	100.00%	100.00%
Forest	0	4	0	0	0	0	0	0	0	4	40.00%	100.00%
River	0	0	27	5	7	0	3	1	0	43	72.97%	62.79%
Grass	0	0	3	1	21	1	3	0	0	29	16.67%	3.45%
Maize	0	2	5	0	26	3	8	7	2	53	48.15%	49.06%
Shrub	0	4	2	0	0	8	3	0	1	18	61.54%	44.44%
Herbacious	0	0	0	0	0	0	5	0	0	5	20.83%	100.00%
Bare	0	0	0	0	0	0	0	4	0	4	33.33%	100.00%
Urban	0	0	0	0	0	1	2	0	8	11	72.73%	72.73%
Column total	19	10	37	6	54	13	24	12	11	186		
Classification	Accuracy	=			**54.84%**							

Table 2 – Error matrix and accuracy assessment for MLC.

4.2.3. NDVI Profile Classification

The divergence statistics are presented in Figure 15. The deflection at class 65 was limited arbitrarily. Figure 16 shows overlay of fieldwork derived times with temporal profiles from ISODATA clustering.

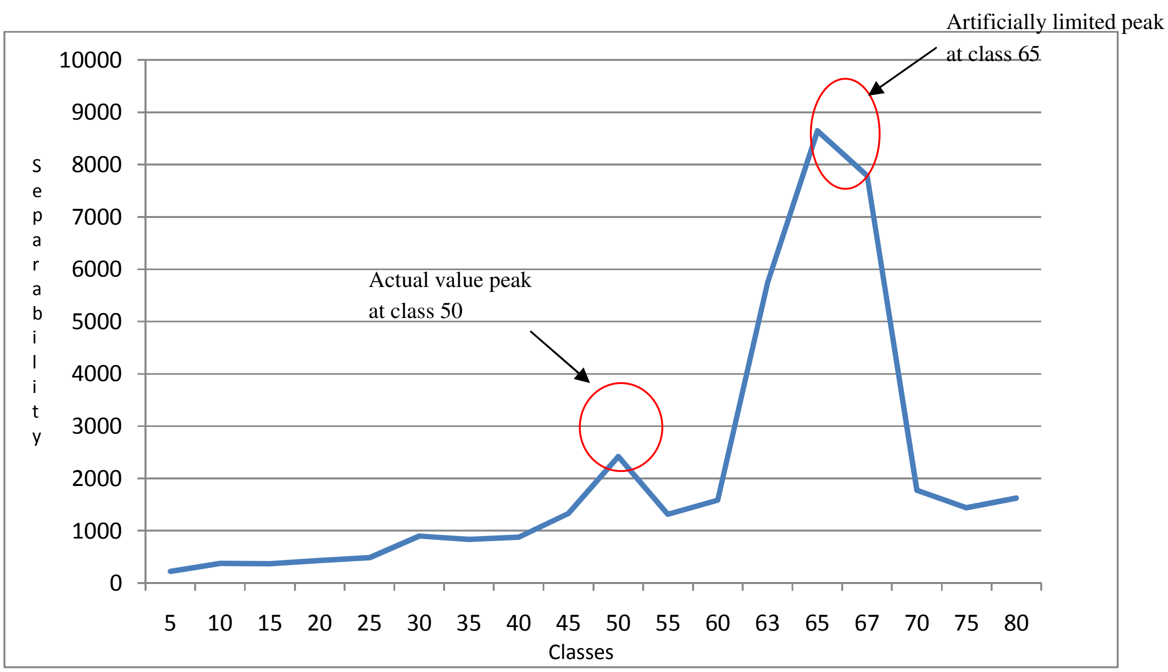

Figure 15 - Average class separability plot. The value at class number 65 was given an arbitrary high value for better scaling, as the original value was more than one million. The peak at 50 was selected instead. Only the average

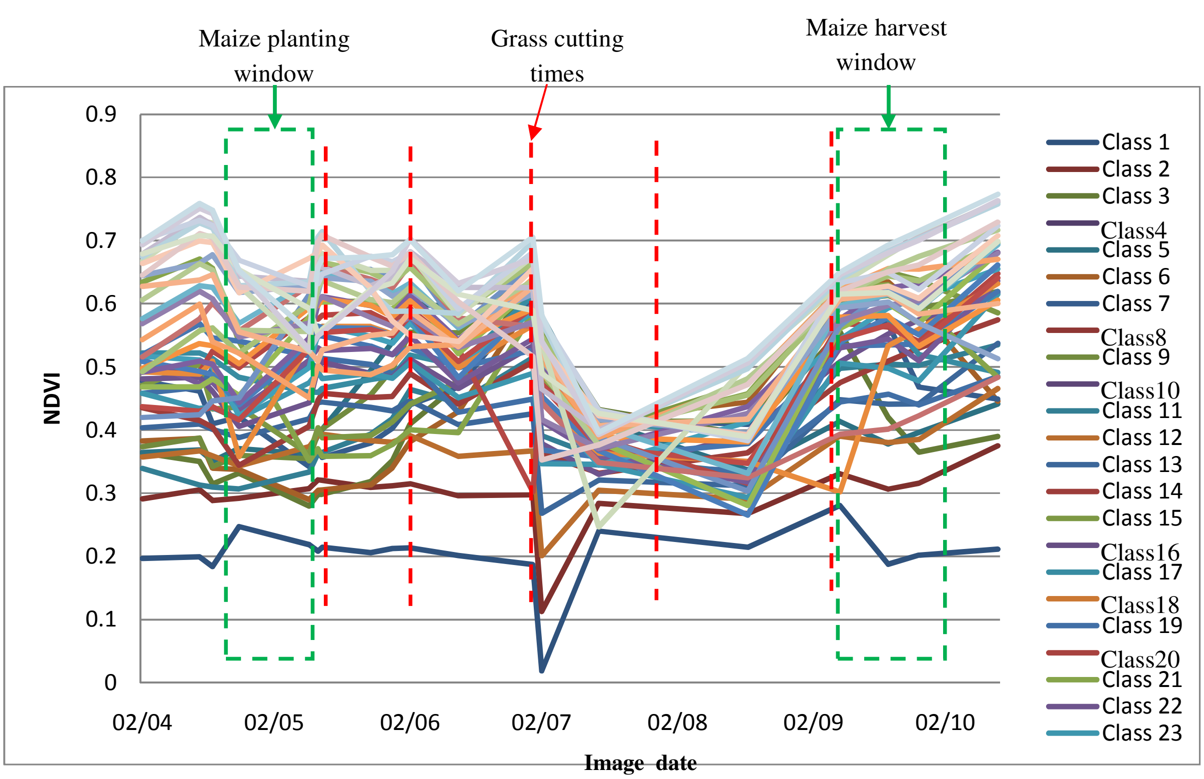

The 19 image stack, NDVI stack and ISODATA cluster images, with field data overlay are presented in Figure 17.

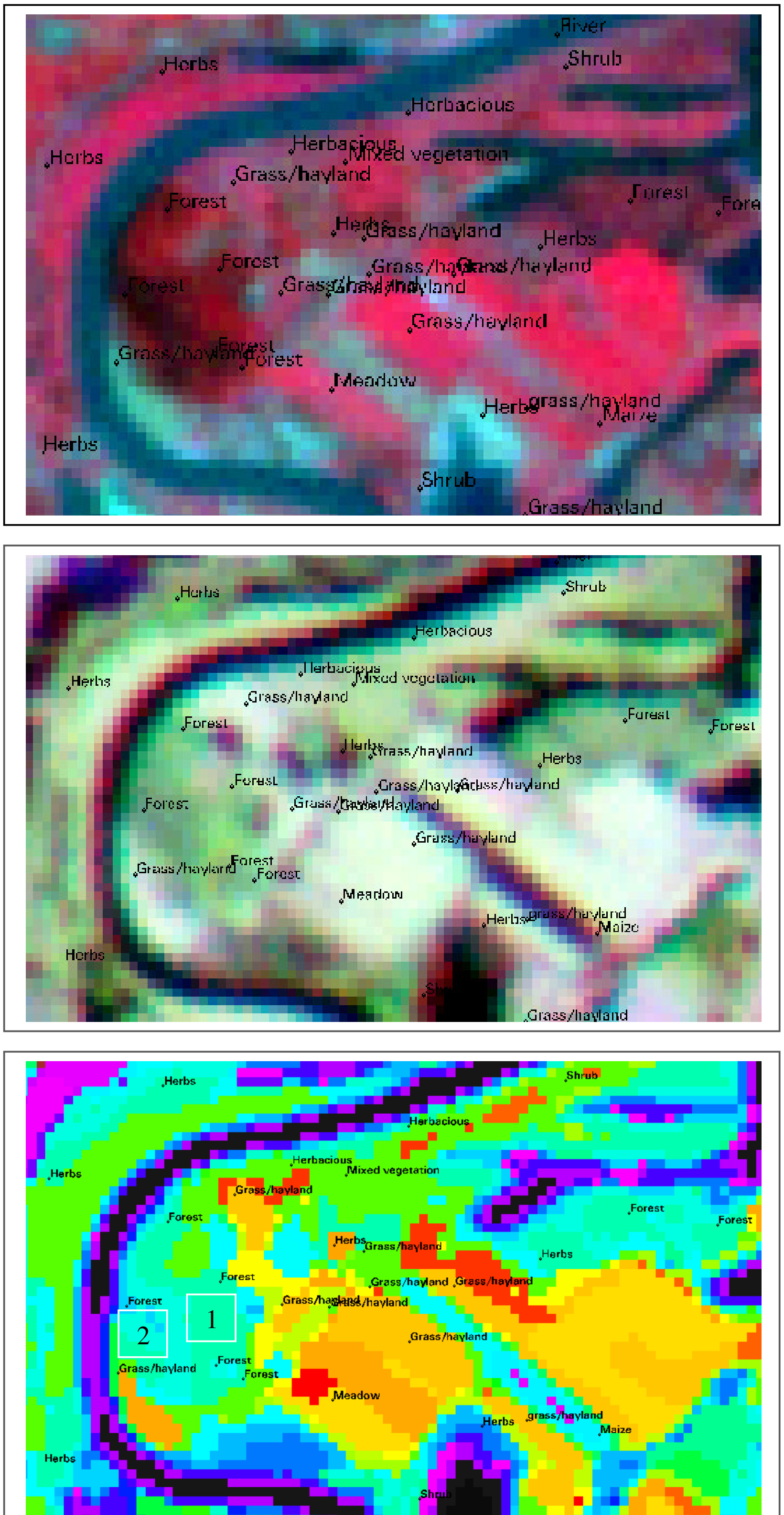

(a)

(b)

(c)

Figure 17 - Image stack of the 19 layers with FCC (a), NDVI Stack (b) and ISODATA cluster (c) of the Fortmond area with sampling points overlaid.

Profiles of known landcover types

Field data was used to plot known landcover classes to observe the general behaviour of the temporal profiles. The results of the temporal NDVI plots against image number are found in Figure 19 to 25 below.

Figure 19 - NDVI temporal profile of herbacious. Two types of herb are captured for the red and black profiles respectively, see picture Plates 17 & 21.

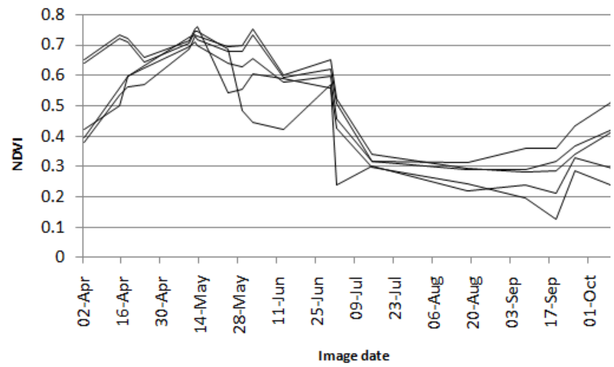

Figure 18 - NDVI temporal profile of bare and temporarily bare areas. The three colour profiles shows temporal state differences

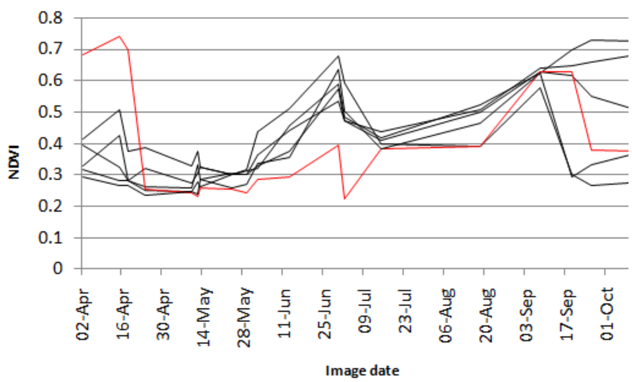

Figure 20 - NDVI temporal profile of Agriculture (Maize) with another slightly varied curve for maize in red.

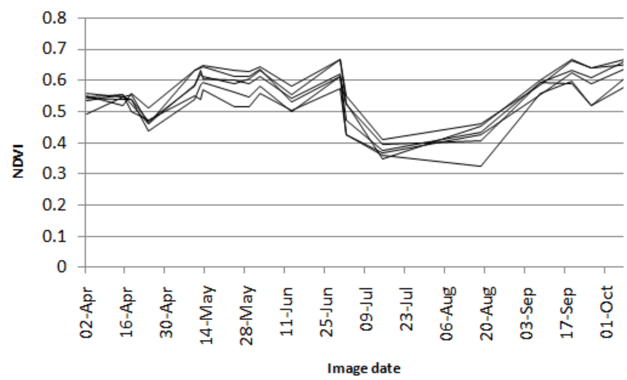

Figure 21 - NDVI temporal profile of forest

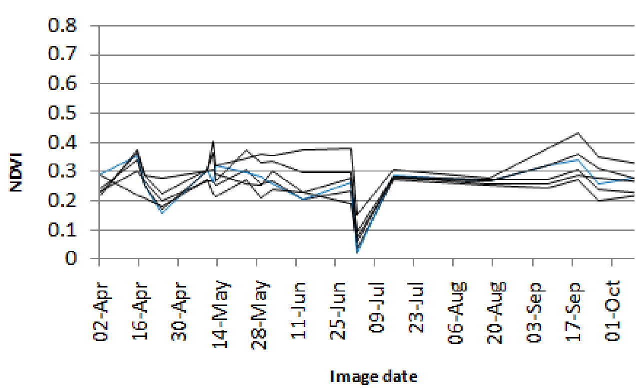

Figure 22 - NDVI temporal profile of water

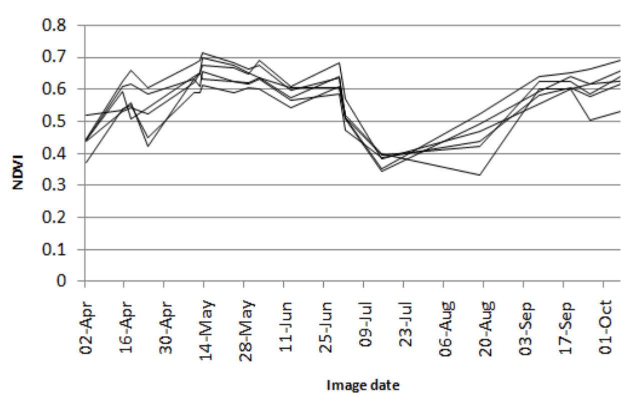

Figure 23 - NDVI temporal profile of shrub land

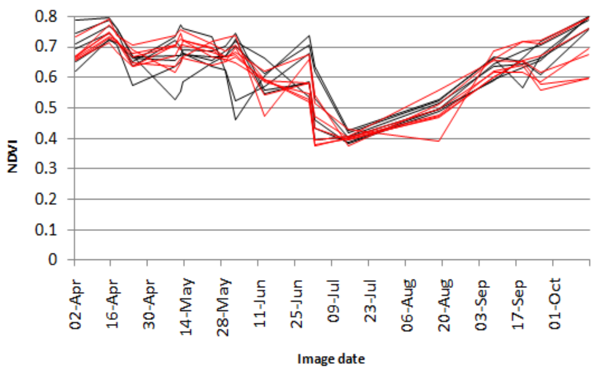

Figure 25 - NDVI temporal profile of grass. Grass include both for haymaking (black) and for meadow(red).

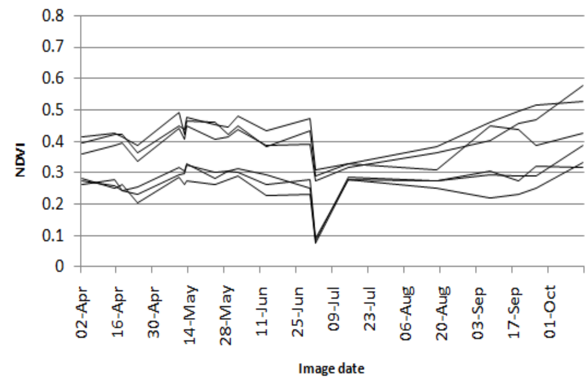

Figure 24 - NDVI temporal profile of urban areas. The red shows an area in the upper section of the image and the black in the lower section

4.3. Leaf Area Index

Despite the fact that there were no coefficients that could be used to relate field measured LAI to NDVI, the measurements were plotted in and their correlation assessed.

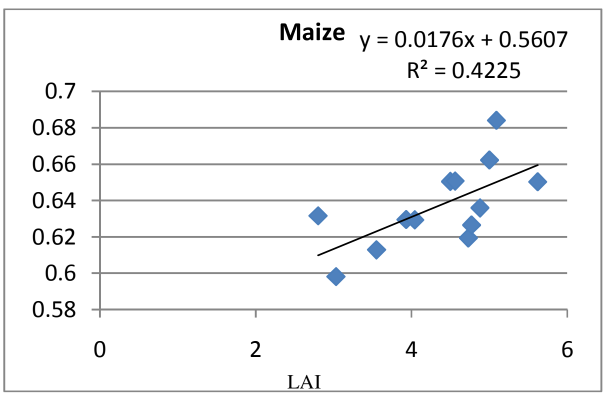

A

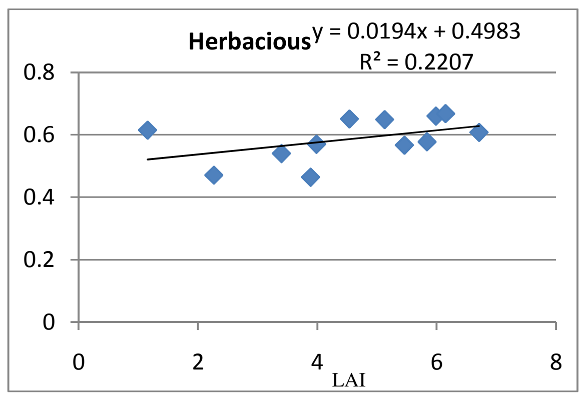

B

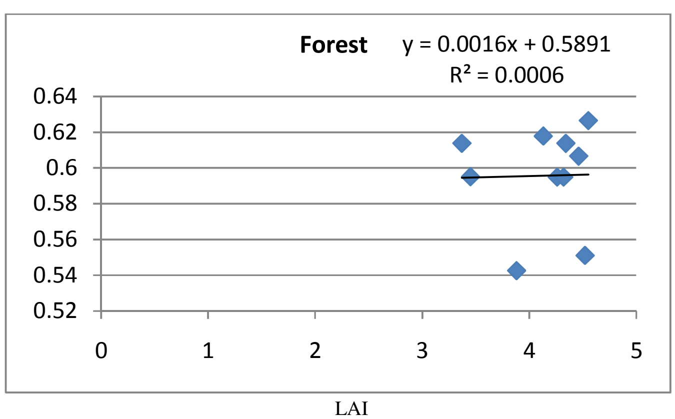

C

Figure 26 - Correlation between LAI and image calculated NDVI for Maize (A), Herbaceous (B) and Forest (C)

5. Discussion

5.1. Fieldwork

An overlay of the farmer responses with the known location temporal profiles for agriculture (maize) the graphs show a significant drop on the temporal profiles at the planting time and at harvesting Figure 11. The graph starts with high NDVI before planting, the values drop at plating time then a steady but fast increase until June where values drop again before increasing from July until September where the harvest is expected. For grass, the “saw tooth” response of the NDVI curve is evident despite not so obvious after July. It is further evident that the response is more pronounced in the hay making plots Figure 12 (in black lines) than in meadows (in red lines). This profile response corresponds well with the information provided by the farmers.

For relating LAI to NDVI, the coefficients that could be used to relate each vegetation type to LAI values were not available. The LAI values that were measured during fieldwork were plotted against image extracted NDVI values with any transformation on the LAI values. The graph for maize shows a poor correlation at $R^2 = 0.42$ while herbaceous vegetation and forest show almost no correlation. The field measurements were also not that significant in terms of population size, with 12, 10, and 13 samples for herbaceous, forest and maize respectively.

5.2. Radiometric and Atmospheric Corrections

The atmospheric corrections were problematic, it is important to perform a proper atmospheric correction process that would make sure that the NDVI values are calculated on accurate reflectance values. The use of ATCOR for atmospheric correction was not successful. The model seemed sensitive to the data format of the DMC images. The model worked inconsistently and either gave errors about low clearline correlation values or just crashed. The model vendor, Geosystems GmbH in Germany also confirmed that they had no experience with the DMC sensors (email communication, November 26th, 2009). They were unable to test the model using the DMC image within the duration of this study, so the errors remain unknown. The alternative to use the TOA was viable but it was noted that the equation used does not correct for atmospheric interference.

5.3. Image Classification

5.3.1. Spectral Angle Mapper

SAM could not differentiate between urban and water. This could be because both areas are made up of very dark pixels and SAM classifies by looking at the spectral angle between the pixels in image space. The small angle between the pixels in the image space means that they would be classified together. From the analysis of the user accuracy, it shows that the shrub and herbs were the least accurately classified at 18.33% and 27.27% respectively and therefore highly influenced the overall accuracy of the results to be low. The next lowest accuracy was bare areas at 55.56%. This is to be expected because in reference to the ecotope maps herbaceous vegetation was found to include a number of different vegetation types with different leaf and stem properties. At some locations natural grass (Pennesetum *purpureum*) was found while at other locations broad leaved perennial vegetation like stinging nettle (Urtica *dioica)* was found. The shrubs also included a number of varying properties with orchards at some places, differing levels of mixture of grass, herb, shrubs and trees. Natural shrubland included a complex combination of vegetation types. In general SAM performed poorly. It could be expected because its strength lies in the existence of varied spectral bands. In a layer stack of 19 images with the same spectral bands, the difference in the variability of the ground objects may not be that significant enough to influence spectral classification in SAM.

5.3.2. Maximum Likelihood Classification

The results of MLC at 54.84% are better than that of SAM at 50.54%. It shows that despite the pixels for urban many of then being dark and some of the areas in the urban area being water, MLC was able to differentiate between water and urban. However there seems to be confusion between grass and agriculture (Maize) in MLC. This could be caused by the impurities in the training set as form the signature histogram, it was realised that there was a lot of overlap between the classes. MLC does not take advantage of the temporal profile of the dataset therefore some cell value combinations may present themselves as similar to other combinations without looking at the order of each combination.

5.3.3. NDVI Profile based

Through visual inspection, the results of ISODATA clustering with 50classes show subtle differences within classes. The forest at the Fortmond area , Figure 17 (c), are 2 is a Pine forest while area 1 is an Oak forest. This is a result of the number of classes that are used for the clustering therefore the algorithm is able to separate classes that could otherwise have been grouped together under other classification methods. This process, corresponds with the method of Townsend and Walsh (2001) where they used a hierarchical classification process. Townsend and Walsh (2001) start form ISODATA clustering and delineate towards a finer classification whereas this methods starts from a detailed clustering to a broader classification. The methods could not be completed due to the complexity and fine differences between the floodplain vegetation studied. A comparison between the work by de Bie *et al*. (2008), Figure 27, shows that this study is limited by the small variation in the phenology and landcover regime, as well as the number of images used to construct differentiable profiles.

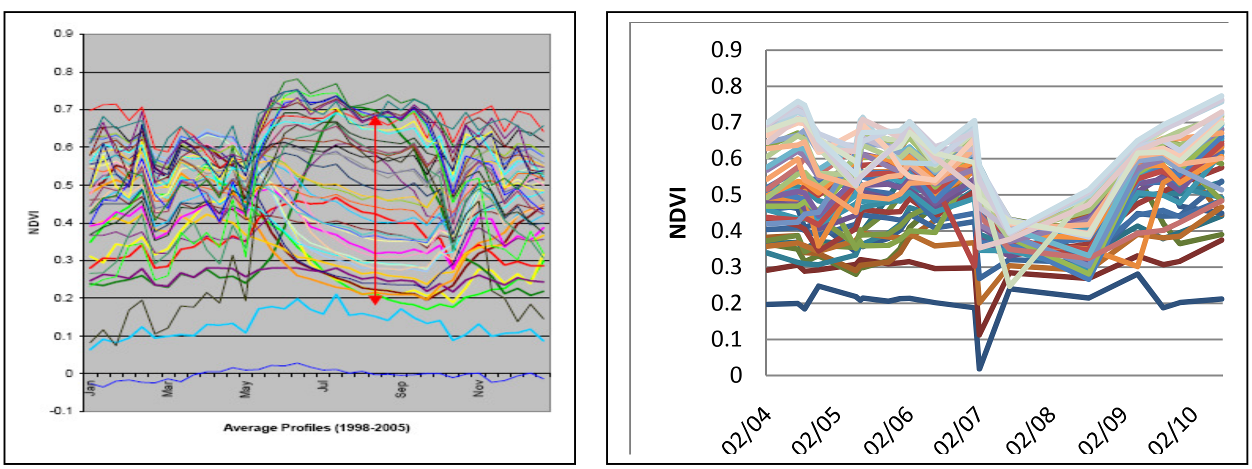

(a) (b)

Figure 27 – Comparison between hypertemporal profiles produced by de Bie et al. (2008) (a) and produced from this study (b)

For the known landcover types using field samples, temporal profiles were produced that evidenced how complex the difference is even for landcovers of the same type. The general response and shape of the curve was be used to evaluate the temporal profile against the landcover type. Considering the general shape of the profiles(Figure 18 to 21), it is observed that maize gives a distinctive signature profile, water gives a profile that is characteristic of minimal change over time whereas forest and grass give almost similar but differentiable profiles. Bare areas and herb give a mixture of profiles and this is to be expected because bare area regimes could have been inconsistent throughout the growing season while herb also included vegetation of different characteristics. However, the temporal profiles show a lot of deflections that may be attributed to artefacts and in general the curves do not follow a strictly expected growth curve for the landcovers displayed. For maize, the deflection is too much as if there has been a double planting. This double cropping not expected in the IJssel floodplain and none of the farmers expressed it with maize.

6. Conclusions & Recommendations

6.1. Conclusions

Based on a 19 layer NDVI stack of the floodplains of the IJssel river, it was clear that NDVI approach is effective in characterising landcover using the temporal dimension of the NDVI stack. The profiles for known locations were able characterise the landcover on that site and produce landcover specific temporal profiles.

Of the three classification methods used MLC performed better than SAM with 54.84% vs 50.54% while ISODATA clustering could only be assessed qualitatively pending the subsequent grouping method. It shows that SAM was not able to take advantage of the layer stack where MLC is known to have limitations (Shafri *et al.*, 2007). The conclusion is SAM is not suitable for a layer stack of identical spectral bands.

The overall objective of the study was not achieved, which was to attain a better classification accuracy than that of the ecotope map at 69%. However the study has shown that floodplain landscape activities can be characterised using the DMC hypertemporal imagery.

6.2. Recommendations

- ❑ Because of the high dynamicity of the IJssel floodplain landcover the study would be enhanced by collection of as many images in a month as possible to be able to use compositing techniques, apply filters and construct a discernible temporal profiles. Otherwise this confirms the need for high temporal properties of satellite imagery.

- ❑ The IJssel floodplain is characterised by patchy landscape. Higher spatial resolution imagery would improve definition of landcover to the resolution comparable to the ecotope maps.

- Higher spectral resolution imagery is required for better prediction of LAI and as well as the use classification methods that take advantage of spectral reflectance differences of floodplain landscape.

- The use of algorithms for NDVI Profile classification must be investigated to support the hypertemporal image classification. Reference profiles must be established to aid algorithm based classification.
- Coefficients that relate LAI to NDVI need to be collect identified for the landcover types found in the IJssel floodplain. A crop calendar would also enhance the hypertemporal classification method.

References

ADDINK, E. A., TEN HAAF, M. E. & DE JONG, S. M. 2009. Monitoring Vegetation Structure in Floodplains for Flood Risk Estimation. *Commission VI, WG VI/4.* Utrecht: Utrecht University.

BRADLEY, B. A. & MUSTARD, J. F. 2008. Comparison of phenology trends by land cover class: a case study in the Great Basin, USA. *Global Change Biology,* 14**,** 334-346.

BREDA, N. J. 2003. Ground-based measurements of leaf area index: a review of methods, instruments and current controversies. *Journal of Experimental Botany,* 54**,** 2403-2417.

COLOMBO, R., BELLINGERI, D., FASOLINI, D. & MARINO, C. M. 2003. Retrieval of leaf area index in different vegetation types using high resolution satellite data. *Remote Sensing of Environment,* 86**,** 120-131.

CONGALTON, R. & GREEN, K. 1999. *Assessing the Accuracy of Remotely Sensed Data: Principles and Practices,* New York, Lewis Publishers.

COTTON, J. A., WHARTON, G., BASS, J. A. B., HEPPELL, C. M. & WOTTON, R. S. 2006. The effects of seasonal changes to in-stream vegetation cover on patterns of flow and accumulation of sediment. *Geomorphology,* 77**,** 320-334.

CROWLEY, G. 2008. DMC Data Product Manual. Guilford: DMC International Imaging (Pty) Ltd.

DANSON, F. M. & PLUMMER, S. E. 1995. Red-edge response to forest leaf area index. *International journal of remote sensing,* 16**,** 183 - 188.

DE BIE, C. A. J. M., KHAN, M. R., TOXOPEUS, A. G., VENUS, V. & SKIDMORE, A. K. 2008. Hypertemporal image analysis for crop mapping and change detection. *In: ISPRS 2008 : Proceedings of the XXI congress : Silk road for information from imagery : the International Society for Photogrammetry and Remote Sensing, 3-11 July, Beijing, China. Comm. VII, WG VII/5. Beijing : ISPRS, 2008. pp. 803-812*.

DE BIE, C. A. J. M. & TOXOPEUS, A. G. unpublished. NDVI Manual - Instruction Material. *Instruction Material.* Enschede: International Institute for Geoinformation Science and Earth Observation (ITC) - Enschede.

DE MOEL, H., VAN ALPHEN, J. & AERTS, J. C. J. H. 2009. Flood maps in Europe – methods, availability and use. *Nat. Hazards Earth Syst. Sci.,* 9**,** 289-301.

DU, Y., TEILLET, P. M. & CIHLAR, J. 2002. Radiometric normalization of multitemporal high-resolution satellite images with quality control for land cover change detection. *Remote Sensing of Environment,* 82**,** 123-134.

EVANS, J. P. & GEERKEN, R. 2006. Classifying rangeland vegetation type and coverage using a Fourier component based similarity measure. *Remote Sensing of Environment,* 105**,** 1-8.

FAN, L., GAO, Y., BRÜCK, H. & BERNHOFER, C. 2009. Investigating the relationship between NDVI and LAI in semi-arid grassland in Inner Mongolia using in - situ measurements. *Theoretical and Applied Climatology,* 95**,** 151-156.

GALIATSATOS, N., DONOGHUE, D. N. M., KNOX, D. & SMITH, K. Unpublished. Radiometric Normalisation of Mutlisensor/Multitemporal Satellite Images with Quality Control for Forest Change Detection.

GEERKEN, R. A. 2009. An algorithm to classify and monitor seasonal variations in vegetation phenologies and their inter-annual change. *ISPRS Journal of Photogrammetry and Remote Sensing,* 64**,** 422-431.

HESSELINK, A. W., STELLING, G. S., KWADIJK, J. C. J. & MIDDELKOOP, H. 2003. Inundation of a Dutch river polder, sensitivity analysis of a physically based inundation model using historic data. *Water Resources Research,* 39.

HORRITT, M. S. 2006. A linearized approach to flow resistance uncertainty in a 2-D finite volume model of flood flow. *Journal of Hydrology,* 316**,** 13-27.

HUAI WEN-XIN, XU ZHI-GANG, YANG ZHONG-HUA & ZENG YU-HONG 2008. Two dimensional analytical solution for a partially vegetated compound channel flow. *Applied Mathematics and Mechanics,* 29**,** 1077-1084.

HUETE, A., DIDAN, K., MIURA, T., RODRIGUEZ, E. P., GAO, X. & FERREIRA, L. G. 2002. Overview of the radiometric and biophysical performance of the MODIS vegetation indices. *Remote Sensing of Environment,* 83**,** 195-213.

JARVELA, J. 2004. Determination of flow resistance caused by non-submerged woody vegetation. *International Journal of River Basin Management,* 2**,** 61-70.

KERLE, N. 2009. Spatial data for Risk Assessment *GeoHazards Data Collection.* Eschede: International Institute for GeoInformation Science and Earth Observation (ITC).

KHAN, M. R., DE BIE, C. A. J. M., KEULEN, V. H., SMALING, E. M. A. & REAL, R. In press. Disaggregating and mapping crop statistics using hypertemporal remote sensing. *International journal of Applied Earth Observation and Geoinformation*.

KHORRAM, S., BIGING, G. S., CHRISMAN, N. R., COLBY, D. R., CONGALTON, R., DOBSON, J. E., FERGUSON, R. L., GOODCHILD, M. F., JENSEN, J. R. & MACE, T. H. 1999. Accuracy assessment of Remote Sensing Devised Change Detection. *American Society for Photogrammetry & Remote Sensing,* ASPRS Monograph**,** 64.

KNOTTERS, M. & BRUS, D. J. In press. Sampling for validation of ecotope maps of floodplains in the Netherlands.

KRUSE, F. A., LEFKOFF, A. B., BOARDMAN, J. B., HEIDEBRECHT, K. B., SHAPIRO, A. T., BARLOON, P. J. & GOETZ, A. F. H. 1993. The Spectral Image Processing System (SIPS) - Interactive Visualization and Analysis of Imaging spectrometer Data. *Remote Sensing of Environment,* 44**,** 145-163.

LI-COR, I. 1992. LAI2000 Plant Canopy Analyser Manual. *In:* NEBRASKA, L.-C. (ed.). Nebraska: LiCor.

LI, C. W. & ZENG, C. 2009. 3D Numerical modelling of flow divisions at open channel junctions with or without vegetation. *Advances in Water Resources,* 32**,** 49-60.

NASA. 2010. *Earth facts* [Online]. Available: http://www.nasa.gov/topics/earth/index.html [Accessed November 28th, 2009 2010].

PAOLINI, L., GRINGS, F., SOBRINO, J. A., MUNOZ, J. C. J. & KARSZENBAUM, H. 2006. Radiometric correction effects in Landsat multi-date/multi-sensor change detection studies. *International journal of remote sensing,* 27**,** 685 - 704.

PONTAILLER, J. Y., HYMUS, J. & DRAKE, B. 2003. Estimation of leaf area index using ground-based remote sensed NDVI measurements: Validation and comparison with two indirect techniques. *Canadian Journal of Remote Sensing,* 23**,** 381-387.

RICHARDS, J. A. & JIA, X. 2006. *Remote sensing digital image analysis : an introduction,* Berlin etc., Springer-Verlag.

SHAFRI, H. Z. M., SUHAILI, A. & MASOR, S. 2007. Performance of Maximum Likelihood, Spectral Angle Mapper, Neural Network and Decision Tree Classifiers in Hyperspectral Image Analysis. *Journal of Computer Science,* 3**,** 419 - 423.

SILVA, W., KLIJN, F. & DIJKMAN, J. 2001. Room for the Rhine Branches in the Netherlands: What the research has taught us. *In:* HYDRAULICS, D. (ed.). Delft: IRMA Sponge.

STRAATSMA, M. 2007. *Hydrodynamic roughness of floodplain vegetation.* PhD Thesis, Utrecht University.

STRAATSMA, M. & ALKEMA, D. 2009. Flood Control 2015; Error propagation in hydrodynamics of lowland rivers due to uncertainty in vegetation roughness parameterization. International Institute of Geo-Information Science and Earth Observation (ITC).

STRAATSMA, M. & MIDDELKOOP, H. 2006. Airborne Laser Scanning as a Tool for Lowland Floodplain Vegetation Monitoring. *Hydrobiologia,* 565**,** 87-103.

STRAATSMA, M. W. & BAPTIST, M. 2008. Floodplain roughness parameterization using airborne laser scanning and spectral remote sensing. *Remote Sensing of Environment,* 112**,** 1062-1080.

SZOSZKIEWICZ, K., KALUZA, T., LESNY, J. & CHOJNICKI, B. Year. Remote Sensing Analysis of the floodplain vegetation structure within a section of the middle vistula river. *In:* International Conference "Towards natural flood reduction strategies", 2003 Warsaw.

TITTEBRAND, A., SPANK, U. & BERNHOFER, C. H. 2009. Comparison of satellite- and ground-based NDVI above different land-use types. *Theoretical and Applied Climatology,* 98**,** 171-186.

TOWNSEND, P. & WALSH, S. 2001. Remote sensing of forested wetlands: application of multitemporal and multispectral satellite imagery to determine plant community composition and structure in southeastern USA. *Plant Ecology,* 157**,** 129-149.

WRIGHT, A., MARCUS, W. A. & ASPINALL, R. 2000. Evaluation of multispectral, fine scale digital imagery as a tool for mapping stream morphology. *Geomorphology,* 33**,** 107-120.

YEN, B. C. 2002. Open Channel Flow Resistance. *Journal of Hydraulic Engineering,* 128**,** 20-39.

ZURITA-MILLA, R., KAISER, G., CLEVERS, J. G. P. W., SHCHNEIDER, W. & SCHAEPMAN, M. E. 2009. Downscaling time series of MERIS full resolution data to monitor vegetation seasonal dynamics. *Remote Sensing of Environment,* 113.

Appendix 1 – Landcover Plates

Plate 2 - Maize canopy

Plate 1 - Maize field

Plate 3 - Maize steam/leaf composition

Plate 4 - Maize understory

Plate 5 - Pine forest canopy

Plate 6 - Beech forest canopy


Plate 8 - Pine forest understory


Plate 7 - Beech forest understory


Plate 10 - Mixed shrub


Plate 9 - Typical Shrub height


Plate 12 - Shrub with grass patch


Plate 11 - Regenerating forest at shrub height

Plate 13 - Grass for haymaking

Plate 14 - Meadow grass with short herbs

Plate 16 - Grass mixed with herbs

Plate 15 - Grass classified as herb in ecotope maps

Plate 17 - herbs of different structures

Plate 18 - herb of homogeneous structure (nettle)


Plate 19 - Herb of mixed structure


Plate 20 - reeds classified as herbs in ecotope maps


Plate 21 - ploughed grass field


Plate 22 - Harvested maize field

Appendix 2 – Questionnaire

Questionnaire (for farming community)

	Record Number:	Plot Number:
Date		
GPS Coordinates	51 _ _ _ _ . _ _ N	06 _ _ _ _ . _ _ E

Landcover/Landuse of the Plot : Area:

1. Name of respondent :

2. Are you the owner of the plot?: No: ☐
Yes: ☐ Since __________(year)

3. Are there animals on the plot?: No: ☐ Yes: ☐

4. If Yes, what type, breed and number of animals:

	breed	number
Cattle		
Sheep		
Horses		
Other		

5. What is the current crop on the field:
Maize making Hay Meadow Other ______________
For Hay specify harvest dates: ____

6. When was this crop planted:
Day/week_______ Month____________ Year ____________

7. When is the planned harvesting time:
Day/week_______ Month____________ Year ____________

8. What was the previous crop on the field:
☐ Maize ☐ Making hay ☐ Meadow Other ____________
____

9. When was this crop planted:
Day/week_______ Month____________ Year ____________

10. When was the crop harvested:
Day/week_______ Month____________ Year ____________

11. Has there been any other farming activity before the ones listed above
If yes name it ____________________________________ Year ___________________________

Appendix 3 – Field data

Site_no_	Class	Landcover	Field_lai	Landcover Description	Date	Interview	X_coord	Y_coord	Classcode
1	Forest	Forest	4.26	Located in Fortmond. Predominantly oak forest with narrow stems and app	8/31/2009		709981.46	5806154.07	2
2	Forest	Forest	3.88	Located in Fortmond, predominantly pine forest with long narrow stems of	8/31/2009		709666.87	5806362.30	2
3	Agriculture	Maize	3.93	Row crop of approximately 0.5m in spacing and 3m height. Whole plot app	8/31/2009	yes	711326.14	5805910.89	8
4	Grass	grass/hayland		Meadow of approximately 15cm height used for hayland. Last cut on or abc	8/31/2009	yes	711070.41	5805961.18	5
5	Herbacious	Herbacious	1.16	Herbacious vegetation of approx. 0.5m height with less than 5% shrubs and	8/31/2009		710244.61	5806856.97	9
6	Herbacious	Herbacious	3.4	Very dense mix of herbacious vegetation and grass. Not much sign of grazir	8/31/2009		710655.74	5806992.61	9
7	Shrub	Mixed vegetation	5.2	dense mix of herbacious vegetation, grass, shrubs and trees. Shrubs are mo	8/31/2009		710436.99	5806821.75	4
8	Bare	ploughed field		Recently ploughed field with rough soil blocks. Next to yard with no Entry s	09/03/2009		715256.32	5792963.41	7
9	Grass	Grass/meadow		Low grass meadow grazed by 11 ponys.	09/03/2009		715309.25	5792810.90	5
10	Agriculture	Maize		Maize field inside the fence over a canal	09/03/2009		715360.00	5792700.61	8
11	Grass	Grass/meadow		Grass meadow field grazed by sheep approx 50mx200m along the fence ne	09/03/2009		715072.34	5792664.70	5
12	Grass	Grass/meadow		Small grass field	09/03/2009		714663.95	5792360.70	5
13	Grass	Grass/meadow		Next to a small lake and a grass field.	09/03/2009		714562.36	5792267.18	5
14	Urban	Urban		Farmers living area with mixed trees	09/03/2009		715038.41	5791932.55	6
15	Grass	Grass/hayland		Grassland for hay making approx. 15cm height. Hay cutting is done here ev	09/03/2009	yes	715136.07	5791932.34	5
16	Agriculture	Maize	4.88	Maize of approximately 2.9m. To be harvested around September 20th.	09/03/2009	yes	715129.36	5791789.48	8
17	Agriculture	Maize	5.62	Maize of approx. 2.8m height at GPS point CO2. Opposite the maize field or	09/03/2009	yes	715154.77	5791615.72	8
18	Herbacious	Herbacious		Dense herbacious crop of approx. 1m height	09/03/2009		715184.41	5791503.40	9
19	Grass	grass/hayland		Grass for hay of about 20cm height. East of the Maize plot at GPS point CO2	09/03/2009	yes	715286.61	5791703.88	5
20	Bare	Bare		Bare land with very short dry grass stumps	09/03/2009		715450.96	5791736.65	7
21	Bare	Bare		Bare land with very short dry grass stumps	09/03/2009		715425.59	5791951.63	7
22	Grass	grass/hayland		short hay grass approx 15cm height. Cutting every 4weeks from May	09/03/2009	yes	715239.39	5791985.85	5
23	Agriculture	Sugarbeet	5	Sugarbeet East of Grass/hayland at site 14. Approximately 40cm height.	09/03/2009		715355.79	5792137.94	9
24	Agriculture	Sugarbeet		Sugarbeet	09/03/2009		715408.69	5792286.16	9
25	Agriculture	Sugarbeet	5.09	Sugarbeet in the same field as site 18. Height Approximately 40cm	09/03/2009		715343.09	5792209.79	9
26	Agriculture	Maize	4.5	Maize close to GPS point C6 with height about 2.4m. Intermittent sunlight c	09/03/2009	yes	715404.39	5792443.02	8
27	Agriculture	Maize		Maize with approx 2.3m height. Light in density to be harvested end of Sep	09/03/2009	yes	715664.63	5792281.72	8
28	Bare	ploughed field		Newly ploughed field	09/03/2009		715603.24	5792434.98	7
29	Grass	grass/hayland		Grass of about 15cm height. Ref 15	09/03/2009	yes	715224.60	5792476.40	5
30	Agriculture	Maize	4.77	Maize of approx 2.8m height at GPS point C9. Harvesting in September	09/03/2009	yes	715063.83	5792374.73	8
31	Grass	Grass/meadow		Grass of about 20cm height	09/03/2009		715063.78	5792498.36	5
32	Agriculture	Maize	4.73	Maize of approximately 2.8m height	09/03/2009	yes	714996.10	5792347.28	8
33	Grass	Grass/herbs		Mixture of grass (40%) and herbs(60%) at height of about 20cm. For sheep	09/03/2009	yes	714890.29	5792360.50	5
34	Grass	Grass/herbs/meadov		Mixture of grass and herbs with cattle grazing	09/03/2009		714592.00	5792067.98	5
35	Grass	Grass/meadow		Meadow grass with access to cattle in location point34 above	09/03/2009		714634.36	5792201.25	5
36	Grass	Grass/herbs		Mixture of grass (50%) and herbs(50%) at height of about 20cm. For sheep	09/03/2009	yes	714731.29	5792023.90	5
37	Grass	Grass/herbs		Mixture of grass at 0.5m height, (70%) and herbs (30%) at 25cm height. Sig	09/04/2009		715205.54	5793305.38	5
38	Grass	Grass/herbs		Grass mixed with herbs	09/04/2009		715294.39	5793367.17	5
39	Grass	Grass/meadow		meadow on the inside of the summer dyke around a deep lake by the mam	09/04/2009		715455.13	5793023.31	5
40	Grass	grass/hayland		Newly ploughed field	09/04/2009		715372.64	5793005.24	5
41	Grass	Grass/meadow		Meadow grass close to the sand pit lake	09/04/2009		715550.40	5793066.45	5
42	Agriculture	Maize		Maize with approx 1.8m height. Light in density	09/04/2009		715486.95	5792856.51	8
44	Herbacious	Herbs/grass		Very rough nature reserve with grass approx. 0.6m height and herbs 0.8m h	09/04/2009		715969.31	5791308.16	9
45	Grass	Grass/meadow		Grassland for making hay on the south of the car only bridge from south de	09/04/2009		715764.04	5791103.17	5
46	Shrub	Shrub		Willow shrub forest within a nature reserve	09/04/2009		716098.36	5791238.05	4
47	Grass	grass/hayland		Grass field used for hay and horse jump training	09/04/2009		716157.59	5790381.87	5
48	Grass	Grass/meadow		Meadow field with signs of grazing	09/04/2009		716292.95	5790366.62	5
49	Grass	Grass/meadow		Grazing field with cattle present	09/04/2009		716409.37	5790391.77	5
50	Grass	grass/hayland		Hayland grass	09/04/2009		716187.23	5790105.82	5
51	Agriculture	Maize		Maize	09/04/2009		716146.99	5789821.15	8
52	Grass	Grass/meadow		Meadow grass with horses	09/04/2009		716335.31	5790184.69	5
53	Bare	Bare		Bare land with ver short dry grass stumps	09/04/2009		716263.39	5789454.21	7
54	Grass	grass/hayland		Hayland grass cut twice a year then converted to meadow for cattle	09/04/2009	yes	716455.86	5789433.67	5
55	Grass	grass/hayland		Hayland grass cut twice a year then converted to meadow for cattle	09/04/2009	yes	716603.98	5789416.76	5
56	Agriculture	Maize		Maize	09/04/2009	yes	716625.13	5789133.65	8
57	Grass	grass/hayland		Hayland grass cut twice a year then converted to meadow for cattle	09/04/2009	yes	716479.11	5789188.52	5
58	Grass	grass/hayland		Hayland grass cut twice a year then converted to meadow for cattle	09/04/2009	yes	716449.55	5789590.44	5
59	Grass	grass/hayland		Hayland grass cut twice a year then converted to meadow for cattle	09/04/2009	yes	716572.23	5789585.78	5
60	Agriculture	Maize		Maize	09/04/2009		716597.65	5790146.05	8
61	Grass	Grass/meadow		meadow grass	09/04/2009		716517.20	5790017.78	5
62	Grass	grass/hayland		Hayland grass with cattle grazing	09/04/2009		716595.57	5789896.46	5
63	Grass	grass/hayland		Hayland grass	09/04/2009		716796.52	5789966.52	5
64	Agriculture	herbs/sugarbeet	3.55	Sugarbeet mixed with herbs of approx 1.2m height, opposite is a Maize fiel	09/04/2009		716697.02	5789787.29	9
65	Agriculture	Maize	4.56	Maize of approximately 2.5m height opposite site 306.	09/04/2009		716912.88	5789824.59	8
66	Agriculture	Maize		Maize area	09/04/2009		716768.99	5789657.89	8
67	Grass	grass/hayland		Grass for hay. Cut 3weeks ago. Cutting every 4-5weeks	09/04/2009	yes	717092.69	5789525.05	5
68	Grass	Grass/meadow		rough meadow grass	09/05/2009		717206.92	5789642.56	5
69	Grass	Grass/herbs		Grass mixed with herbs. Rough meadow, ungrazed.	09/06/2009		717329.61	5789232.48	5
70	Agriculture	Maize		Maize	09/07/2009		717067.30	5789283.35	8
71	Bare	Bare		Bare land between grass and maize with a row of boundary vegetation	09/08/2009		716946.73	5789431.77	7
72	Grass	Grass/meadow		Meadow grass	09/09/2009		717422.72	5789617.51	5
73	Grass	Grass/meadow		Meadow grass	09/10/2009		717377.38	5789431.73	5
74	Grass	Grass/meadow		Meadow grass	09/11/2009		717515.80	5789437.81	5
75	Grass	grass/hayland		Grass for haymaking	09/12/2009		717596.18	5789002.49	5
76	Grass	grass/hayland		Grass for haymaking	09/01/2010		717617.36	5789258.49	5
77	Grass	Grass/meadow		Grass for meadow with cattle grazing	09/02/2010		717792.93	5789112.50	5
78	Agriculture	Maize		Maize field. Quite dense	09/03/2010		715992.57	5790529.49	8
79	Agriculture	Maize		Maize field. Quite dense	09/04/2010		715791.60	5790518.49	8
80	Grass	grass/hayland		Grassland for hay making and meadow	09/05/2010		715990.44	5790301.06	5
81	Grass	grass/hayland		Grassland for hay making and meadow	09/06/2010		715800.04	5790186.94	5
82	Grass	Grass/meadow		Grassland for sheep grazing	09/07/2010		715787.40	5789951.37	5
83	Agriculture	Maize	4.04	Maize of approximately 2.5m height.	09/08/2010		715540.38	5792697.33	8
84	Agriculture	Maize	2.8	Maize of approximately 2.3m height	09/09/2010		715479.23	5792867.31	8
85	Grass	Grass/meadow		Regularly grazed meadow with scattered herbs making 25%. Grass of about	09/08/2009		717492.48	5782751.46	5
86	Grass	Grass/hayland		Grass hayland for sheep. Height of about 60cm, to be cut today on Septemb	09/08/2009		717492.48	5782751.46	5
87	Grass	Grass/meadow		Short meadow grass with a small water canal of about 1m width passing in	09/08/2009		717691.57	5783547.68	5
88	Grass	Grass/meadow		Open area with cattle present and grazing. 60% grass and about 40% short	09/08/2009		717936.10	5784509.66	5

89	Grass	Grass/meadow		Meadow area in the same location as site 39.	09/08/2009		717901.30	5784773.22	5
90	Grass	Grass/meadow		Meadow grass mowed with even height.	09/08/2009		717876.47	5785138.59	5
91	Grass	Grass/meadow		Rough meadow grass	09/08/2009		718032.11	5785188.87	5
92	Grass	Grass/meadow		Rough meadow grass with a lot of geese. Grass is about 15cm and herbs ar	09/08/2009		717732.43	5785372.85	5
93	Herbacious	herbs/shrubs		Dominated by herbs. Some trees and a clump of meadow bush closest to th	09/08/2009		717462.50	5785472.38	9
94	Shrub	Mixed vegetation		Grass about 40%, herbs 20%, shrubs 30% and scattered trees. Willows, reec	09/08/2009		717257.23	5785617.09	4
95	Grass	Grass/hayland		Newly cut grassland. Opposite on the other side of the dyke is Maize field. I	09/08/2009		716947.61	5785884.21	5
96	Grass	Grass/meadow		Rough Meadow	09/08/2009		716949.27	5786183.91	5
97	Grass	Grass/hayland		opposite sections of grassland with line vegetation	09/08/2009		716505.54	5785923.91	5
98	Shrub	Mixed vegetation		Mixed vegetation with 40% grass, herbs 5%, shrubs 30%, trees 15%. Willow	09/08/2009		716233.98	5785924.30	4
99	Shrub	Mixed vegetation		Mixed vegetation with 40% grass, herbs 5%, shrubs 30%, trees 15%. Willow	09/08/2009		716320.05	5785957.02	4
100	Agriculture	Maize		Maize fields outside the dyke all the way to the church building.	09/08/2009		715798.47	5785944.30	8
101	Grass	Grass/hayland		Four grass fields separated by line vegetation.	09/08/2009		715368.03	5785805.27	5
102	Shrub	Mixed vegetation	4.92	cut vegetation with oak stumps and short succession oak trees. Grass of ab	09/08/2009		715088.23	5786429.11	4
103	Agriculture	Maize	3.03	Maize field opposite the mixed vegetation field with height about 1.8m	09/08/2009		715142.87	5786365.76	8
104	Forest	Forest	4.55	Forest with minimal understory growth. Mixture of oak and birch.	10/06/2009		717496.59	5791004.36	2
105	Grass	Meadow		Meadow with grass of about 5cm and herbs of about 40cm. Being grazed b	10/06/2009		718099.59	5789614.59	5
106	Forest	Forest	4.34	Forest near Gorssell. Under canopy is covered by leaf litter. Mainly birch fo	10/06/2009		717964.63	5788495.69	2
107	Herbacious	Herb	6.71	Herbs and tall reeds/grass along a marsh floodplain	10/06/2009		716996.01	5787887.90	9
108	Shrub	Mixed vegetation		Mixed herb, grass and shrubs	10/06/2009		716654.31	5787817.08	4
109	Herbacious	Herb	5.13	Herbs and tall reeds/grass along a marsh floodplain	10/06/2009		716348.98	5787979.79	9
110	Grass	Meadow		Meadow grass with cows grazing	10/06/2009		716291.55	5787588.32	5
111	Grass	Meadow		Meadow grass on an undulating terrain	10/06/2009		716257.09	5787516.53	5
112	Grass	Grass/hayland		Hay grass at about 15cm	10/06/2009		716451.39	5787451.45	5
113	Grass	Meadow		Meadow grass on an undulating terrain	10/06/2009		716494.46	5787545.25	5
114	Herbacious	Herbs	4.54	Sugarbeet next to a harvested maize field	10/06/2009		717607.62	5787930.02	9
115	Bare	Bare		Recently harvested maize field	10/06/2009		717581.78	5787891.73	7
116	Agriculture	Maize		Planted in May 17th and harvested in October 5th.	10/06/2009	yes	716623.68	5789068.06	8
117	Grass	Grass/hayland		Grass cut in June and August around 20th, then converted to meadow	10/06/2009	yes	716521.26	5788689.03	5
118	Herbacious	Herbs		Very short herbacious crop with leaves less than 15cm	10/06/2009		716521.26	5788429.65	9
119	Shrub	Shrub	1.6	Pears and Apple Orchard	10/06/2009		716287.72	5788572.26	4
120	Herbacious	Herbs	6.15	Thick herbacious vegetation mainly stinging nettle. Approximately 1metre h	10/05/2009		711045.67	5803671.54	9
121	Herbacious	Herbs	5.99	Thick herbacious vegetation mainly stinging nettle. Approximately 0.9 metr	10/05/2009		710903.50	5804089.06	9
122	Herbacious	Natural Grass	5.46	Tall natural grass, not grazed. Approximately 1.3m tall	10/05/2009		711090.49	5803982.76	9
123	Bare	Bare		harvested field	10/05/2009		711054.63	5804206.89	7
124	Shrub	Mixed Vegetation	2.87	Mixed shrub, and grass. Mainly hawthorne	10/05/2009		710818.97	5804258.12	4
125	Bare	Bare		Just harvested probably on this day.	10/05/2009		710706.27	5804464.32	7
126	Bare	Bare		Mulched with grass to almost bare	10/05/2009		710680.65	5804505.31	7
127	Shrub	Orchard		A small orchard within the dyke	10/05/2009		710623.02	5804438.71	4
128	Agriculture	Maize		Maize field, the owner not comfortable with fied measurements	10/05/2009		710065.39	5804941.76	8
129	Grass	Grass		grass for hay cut every month for making pellets.	10/05/2009		710279.42	5804809.70	5
130	Grass	Grass		grass for hay cut every month for making pellets.	10/05/2009		709965.21	5805087.48	5
131	Bare	Bare		bare area, part of the government program for constructing a river bypass	10/05/2009		709858.20	5805133.02	7
132	Bare	Bare		bare harvested area	10/05/2009		709949.27	5805262.80	7
133	Herbacious	Herbs	5.84	herbacious vegetation with tall grass, approximately 1.8m tall	10/05/2009		709373.22	5805809.26	9
134	Herbacious	Herbs		herbacious vegetation with tall grass	10/05/2009		709393.71	5806808.81	9
135	Herbacious	Herbs		herbacious vegetation with tall grass	10/05/2009		709794.44	5807134.41	9
136	Grass	Meadow		Rough mixture of meadow and herbs, next to the ferry.	10/05/2009		712754.40	5809119.85	5
137	Forest	Forest	4.52	Forest with thick under canopy. Inaccessible to propoer LAI measurements.	10/05/2009		711741.19	5806647.15	2
138	Forest	Forest	3.45	Forest with overgrown under canopy	10/05/2009		711431.53	5806688.14	2
139	Herbacious	Herbs	3.99	Herb of 1.6m tall with grass of about 0.8metre tall	10/05/2009		711119.60	5806526.48	9
140	Herbacious	Herbs	3.89	Herbs of approximately 0.8metres tall	10/05/2009		710914.67	5805939.04	9
141	Herbacious	Herbs	2.27		10/15/2009		711473.62	5803421.29	9
142	Urban	Urban			10/15/2009		711676.91	5803751.21	6
143	Shrub	Shrub			10/15/2009		710693.80	5805684.10	4
144	Forest	Forest	3.37		10/15/2009		710075.61	5806105.67	2
145	Grass	Grass/hayland		Grass for hay cut twice a year in June and July	10/15/2009	yes	710043.95	5806752.18	5
146	Grass	Meadow		Grass for cows	10/15/2009	yes	710388.87	5806030.68	5
147	Grass	Grass/hayland		Grass for hay cut twice a year in June and July	10/15/2009	yes	711067.05	5805589.12	5
148	Grass	Grass/hayland		Grass cut twice a year in June and August	10/15/2009	yes	710520.51	5806428.92	5
149	Grass	Grass/hayland		Grass cut twice a year June and August	10/15/2009	yes	710378.87	5806357.27	5
150	Grass	Grass/hayland		Grass cut twice a year June and August	10/15/2009	yes	710498.85	5806553.89	5
151	Herbacious	Herbs			10/15/2009	yes	710393.87	5806575.56	9
152	Grass	Grass/hayland		Grass for making hay cut in May, July then August	10/15/2009	yes	710658.81	5806237.30	5
153	Grass	Grass/hayland		Grass for making hay cut in May, July then August	10/15/2009	yes	710817.11	5806432.26	5
154	Grass	Grass/hayland		Grass for making hay cut in May, June, then August	10/15/2009	yes	710210.58	5806365.60	5
155	Grass	Grass/hayland		Grass for making hay cut in May, June , then August	10/15/2009	yes	709635.71	5806125.66	5
156	Forest	Forest	4.32		10/15/2009		709810.67	5806657.20	2
157	Forest	Forest	4.46		10/15/2009		709993.96	5806447.25	2
158	Shrub	Shrub		Swampy area with overgrown underbrush	10/15/2009		711206.62	5807154.05	4
159	Shrub	Shrub		Swampy area with overgrown underbrush	10/15/2009		712296.86	5807422.54	4
160	Urban	Urban		Urban	10/16/2009		714316.51	5794872.52	6
161	Urban	Urban		Urban	10/16/2009		715191.75	5794923.02	6
162	Urban	Urban		Urban	10/16/2009		718835.78	5794047.78	6
163	Urban	Urban		Urban	10/16/2009		712077.92	5803119.97	6
164	Urban	Urban		Urban	10/16/2009		719652.11	5782476.10	6
165	Urban	Urban		Urban	10/16/2009		718600.14	5782476.10	6
166	Urban	Urban		Urban	10/16/2009		720906.06	5780035.52	6
167	Urban	Urban		Urban	10/16/2009		719626.86	5781196.90	6
168	Deepwater	Deepwater		Deepwater	10/16/2009		716083.82	5787146.85	1
169	Deepwater	Deepwater		Deepwater	10/16/2009		717876.38	5785564.68	1
170	Deepwater	Deepwater		Deepwater	10/16/2009		717354.60	5785741.41	1
171	Deepwater	Deepwater		Deepwater	10/16/2009		717581.83	5789999.79	1
172	Deepwater	Deepwater		Deepwater	10/16/2009		716336.29	5790841.37	1
173	Deepwater	Deepwater		Deepwater	10/16/2009		715772.44	5792886.40	1
174	Deepwater	Deepwater		Deepwater	10/16/2009		711160.60	5805030.35	1
175	Deepwater	Deepwater		Deepwater	10/16/2009		710967.03	5805434.31	1
176	Deepwater	Deepwater		Deepwater	10/16/2009		712010.59	5807285.78	1
177	Deepwater	Deepwater		Deepwater	10/16/2009		716504.61	5790731.96	1
178	River	River		River	10/16/2009		718314.00	5784470.63	3

179	River	River	River	10/16/2009	718112.02	5785724.58	3
180	River	River	River	10/16/2009	715789.27	5787138.43	3
181	River	River	River	10/16/2009	717674.40	5788585.94	3
182	River	River	River	10/16/2009	717893.21	5789924.05	3
183	River	River	River	10/16/2009	715873.43	5791859.68	3
184	River	River	River	10/16/2009	711480.40	5804045.71	3
185	River	River	River	10/16/2009	710790.30	5805181.84	3
186	River	River	River	10/16/2009	711177.43	5807268.95	3

Appendix 4 – Fieldwork farming activity response

Field	Area	Crop	Apr	May	Jun	Jul	Aug	Sep	Oct
1	Fortmond	Grass		1	1		1		
2	Fortmond	Grass		1		1	1		
3	Fortmond	Grass		1	1	1	1		
4	Fortmond	Grass		1		1	1		
5	Fortmond	Grass			1		1		
6	Fortmond	Grass			1		1		
7	Fortmond	Grass			1		1		
8	Fortmond	Grass			1	1			
9	Fortmond	Grass			1	1			
10	Gorssel	Grass			1		1		
11	Deventer	Grass		1	1	1	1	1	
12	Fortmond	Grass		1	1		1		
13	Deventer	Grass		1	1	1	1	1	
14	Gorssel	Grass		1		1	1	1	
15	Gorssel	Grass		1		1			
16	Deventer	Grass		1	1	1	1	1	
17	Gorssel	Grass			1		1		
18	Gorssel	Grass			1		1		
19	Gorssel	Grass			1		1		
20	Deventer	Grass		1	1		1	1	
21	Gorssel	Grass			1		1		
22	Gorssel	Maize		1					1
23	Deventer	Maize		1				1	
24	Deventer	Maize		1				1	
25	Deventer	Maize		1				1	
26	Deventer	Maize		1				1	
27	Deventer	Maize		1				1	
28	Deventer	Maize		1				1	

Table 3 - the table shows harvesting cycle for grass while for maize the dates are planting and harvesting times

Appendix 5 – Field LAI vs NDVI

Item no.	CLASS	LANDCOVER	FIELD Measured LAI	Image generated NDVI
1	Herbacious	Herbacious	1.16	0.614852
2	Shrub	Shrub	1.60	0.636577
3	Herbacious	Herbs	2.27	0.470426
4	Agriculture	Maize	2.80	0.631565
5	Shrub	Mixed Vegetation	2.87	0.580491
6	Agriculture	Maize	3.03	0.598108
7	Forest	Forest	3.37	0.613880
8	Herbacious	Herbacious	3.40	0.539887
9	Forest	Forest	3.45	0.595151
10	Agriculture	herbs/sugarbeet	3.55	0.612866
11	Forest	Forest	3.88	0.542489
12	Herbacious	Herbs	3.89	0.463964
13	Agriculture	Maize	3.93	0.629530
14	Herbacious	Herbs	3.99	0.569640
15	Agriculture	Maize	4.04	0.629364
16	Forest	Forest	4.13	0.617952
17	Forest	Forest	4.26	0.594925
18	Forest	Forest	4.32	0.594925
19	Forest	Forest	4.34	0.613900
20	Forest	Forest	4.46	0.606726
21	Agriculture	Maize	4.50	0.650461
22	Forest	Forest	4.52	0.551032
23	Herbacious	Herbs	4.54	0.650461
24	Forest	Forest	4.55	0.626611
25	Agriculture	Maize	4.56	0.650685
26	Agriculture	Maize	4.73	0.619359
27	Agriculture	Maize	4.77	0.626518
28	Agriculture	Maize	4.88	0.635889
29	Shrub	Mixed vegetation	4.92	0.608762
30	Agriculture	Sugarbeet	5.00	0.662250
31	Agriculture	Sugarbeet	5.09	0.684127
32	Herbacious	Herb	5.13	0.648379
33	Shrub	Mixed vegetation	5.20	0.595701
34	Herbacious	Natural Grass	5.46	0.566411
35	Agriculture	Maize	5.62	0.650258
36	Herbacious	Herbs	5.84	0.577311
37	Herbacious	Herbs	5.99	0.659827
38	Herbacious	Herbs	6.15	0.667406
39	Herbacious	Herb	6.71	0.607692

Table 4 - Field measured LAI measurements and translation to NDVI